SEVERE DERMATOPHYTOSIS IN PERSIAN CATS: A MULTI-OMICS APPROACH TO UNRAVELING PATHOGENESIS

A Dissertation

by

ALEXANDRA NICHOLE MYERS

Submitted to the Office of Graduate and Professional Studies of
Texas A&M University
in partial fulfillment of the requirements for the degree of

DOCTOR OF PHILOSOPHY

Chair of Committee,	Aline Rodrigues Hoffmann
Co-Chair of Committee,	William J. Murphy
Committee Members,	Sara D. Lawhon
	Alison B. Diesel
	Albert Mulenga
Head of Department,	Ramesh Vemulapalli

August 2021

Major Subject: Biomedical Sciences

ABSTRACT

In recent years, a surge in cases of chronic and treatment resistant dermatophytosis (ringworm) in humans has brought renewed interest in studying this disease. Persian cats are prone to developing a severe form of dermatophytosis characterized by extensive and chronic infections not seen in other cat breeds. Identifying a cause for severe disease in Persian cats may inform our understanding of pathogenesis in both animals and humans.

We took a two-part, next-generation-sequencing (NGS)-based approach to identify a cause for severe dermatophytosis in Persian cats. First, we examined the Persian cat microbiota using 16S and ITS amplicon sequencing and analysis. We found that cutaneous bacterial and fungal populations were not overtly different between case and control cats with the exception of the presence of the dermatophyte *Microsporum canis*. The microbiota diversity and composition did not appear to contribute significantly to defense against dermatophytes, although more work may be needed to confirm this finding.

Second, we sought to identify genetic variation associated with severe dermatophytosis using whole genome sequencing (WGS), genome-wide association study (GWAS), tests of natural selection, and functional assays. WGS and GWAS revealed a highly divergent, disease-associated haplotype on chromosome F1 containing the S100 family of genes. In particular, *S100A9* contained thirteen nonsynonymous variants between cases and controls. Comparison of the divergent Persian cat *S100A9*

haplotypes with those of wild felids indicated that the disease-associated haplotype may have been introgressed into the ancestor of the sand cat and domestic cat from a wild felid ancestor. The haplotype then appears to have been maintained under balancing selection. We demonstrated that S100A8/S100A9 (an antimicrobial peptide known as calprotectin) expression is upregulated in the feline epidermis during dermatophytosis, confirming a role of S100A9 in the immune response to dermatophytes.

Studies show that amino acid substitutions in antimicrobial peptides (AMPs) can alter pathogen specificity. Given that this divergent haplotype has been maintained in domestic cats, it may have beneficial effects against other feline pathogens. Calprotectin proteins represent a promising therapy for dermatophytosis in humans and animals, especially if particular amino acid substitutions can be shown to heighten antimicrobial activity against these ubiquitous fungal pathogens.

DEDICATION

To Bob, whose squishy face brought this upon us all.

ACKNOWLEDGEMENTS

I would first like to thank my committee chair and co-chair, Drs. Aline Rodrigues Hoffmann and William Murphy, for their guidance and mentorship throughout the course of my research. Dr. Rodrigues created the perfect opportunity for me to pursue my scientific interests and encouraged me every step of the way. She has been the understanding mentor and friend we all need when life gets tough, academically or otherwise. Dr. Murphy is truly an advocate for his students and for good science. I cannot thank him enough for creating a supportive lab environment that encouraged team-work, critical thinking, productivity, and good times. He has greatly broadened my perspective as a scientist, which in turn has made me a better veterinarian and pathologist. I hope that someday I will have the opportunity to pass on at least some of what I've learned from both of these amazing mentors.

I would like to thank my committee members, Drs. Alison Diesel, Sara Lawhon, and Albert Mulenga, who provided much needed support and discussion. They each opened my eyes to new ideas and helped advance this dissertation research in unique ways. Drs. Dominique Wiener, Katia Groch, and Dimitrios Kontoyiannis also provided helpful insights and discussion.

This work could not have been completed without the veterinarians, technicians, and cat owners who helped submit samples. I would especially like to thank Amanda Friedeck and Drs. Mary McCaine, Cynthia McManis, Cheryl Stanley, Rendina

McFadden, Massimo Beccati, Silvia Auxilia, Olga Sjatkovskaja, Sasha Gibbons, Charles Bradley, and Warren Joubert for taking the time to contribute to this research.

I very certainly would not have made it this far without the support of my labmates Dr. Caitlin Older, Dr. Nicole Foley, Kevin Bredemeyer, Andrew Harris, Dr. Wesley Brashear, Dr. Paula Giaretta, Dr. Jeann Leal, Dr. Mayane Faccin, Anna Blick, and Dr. Courtney Meason Smith. I learned so much more from you all than just how to science: important skills like how to eat spicy food, but also how to be a better friend and teammate. You all are amazing.

Special thanks to Dr. Mark Johnson for being that mentor you can talk to about anything anytime and always feel better about life afterward. Thanks for getting me here and helping me make all the right choices.

I want to thank my parents Dean and Catherine Myers for literally everything. Just everything. Thank you. And to my husband Brian: you absolutely deserve an award for weathering this academic journey with me for over a decade. Thank you for being here and taking care of me through all of it.

CONTRIBUTORS AND FUNDING SOURCES

Contributors

This work was supervised by a dissertation committee consisting of Dr. Aline Rodrigues Hoffmann (advisor) of the Department of Veterinary Pathobiology, Dr. William Murphy (co-advisor) of the Department of Veterinary Integrative Biosciences, Dr. Sara Lawhon of the Department of Veterinary Pathobiology, Dr. Alison Diesel of the Department of Small Animal Clinical Sciences, and Dr. Albert Mulenga of the Department of Veterinary Pathobiology.

The immunohistochemistry in Section 3 was performed by Dr. Andy Ambrus of the Texas A&M University CVMBS Core Histology Lab.

All other work conducted for the dissertation was completed by Alexandra Myers, with significant guidance and consideration from Drs. William Murphy and Aline Rodrigues Hoffmann.

Funding Sources

Graduate study was supported by a postdoctoral fellowship from the National Institutes of Health under award number T32OD011083.

This work was made possible by a Miller Trust Grant from The Winn Feline Foundation under Grant Number MT16-015. Its contents are solely the responsibility of the authors and do not necessarily represent the official views of the Winn Feline Foundation.

NOMENCLATURE

AMP	Antimicrobial peptide
ANOSIM	Analysis of Similarities
ASV	Amplicon sequence variant
DLH	Domestic longhair cat
DSH	Domestic shorthair cat
DTM	Dermatophyte test media
EMMAX	Efficient mixed-model association eXpedited
FFPE	Formalin-fixed paraffin-embedded
GWAS	Genome-wide association study
IHC	Immunohistochemistry
IL	Interleukin
ITS	Internal transcribed spacer
NGS	Next-generation sequencing
PCoA	Principal coordinates analysis
qPCR	Quantitative polymerase chain reaction
SNP	Single nucleotide polymorphism
SNV	Single nucleotide variant
WGS	Whole-genome sequencing

TABLE OF CONTENTS

Page

LIST OF FIGURES

Page

LIST OF TABLES

Page

1. INTRODUCTION

1.1. Motivation and Aims

Dermatophytes are highly successful fungal pathogens affecting the skin, nails, and hair of humans and animals on every continent worldwide. The infections caused by this group of fungi go by a variety of common names, including 'ringworm,' 'tinea,' 'athlete's foot,' 'jock itch,' and others, but the overarching term for this disease is dermatophytosis. It is estimated that up to $^{1}/_{8}$ or even $^{1}/_{4}$ of the world's population is affected with fungal skin disease, predominantly caused by dermatophytes (Havlickova et al. 2008; Global Burden of Disease Study 2013 Collaborators 2015; Bongomin et al. 2017). Despite the high worldwide prevalence of this disease, the virulence mechanisms and pathogenesis have gone surprisingly understudied.

In recent years, an alarming increase in incidence of chronic dermatophytosis resistant to typical treatment has been observed, particularly in India (Nenoff et al. 2019; Narang et al. 2019; Das et al. 2020; Patel et al. 2020). These infections are beginning to be reported elsewhere in the world (Saunte et al. 2021). A flurry of scientific activity has begun in order to improve our understanding of how dermatophytosis occurs and how the immune system combats it (Gräser et al. 2018). An improved understanding of these mechanisms will allow researchers to design new, targeted therapies to thwart these pathogens or augment host immunity.

This was not the sole motivation for this dissertation research however. This research was also motivated by questions that have arisen in the veterinary community

about the reason for the higher incidence and severity of dermatophytosis in Persian cats than in other breeds. Many veterinary textbooks, case reports, and reviews have speculated on possible reasons for this predisposition (Moriello et al. 2017; Scott et al. 2001; Chang et al. 2011; Nuttall et al. 2008; Nitta et al. 2016). Most have suggested or assumed a genetic predisposition, but prior to this research, there has been no formal investigation into the matter. It was also postulated that Persian cats might carry dermatophytes asymptomatically on their hair coat more often than other breeds (Nitta et al. 2016). These questions have been of great personal interest to many cat owners/breeders and veterinarians who deal with the disease on a regular basis. One veterinarian and Persian cat breeder described dermatophytosis as "the Persian cat nemesis" (Susan Randlett-Price, personal communication). We felt that investigating this problem in Persian cats and identifying potential reasons for severe infections could lend insight into the pathogenesis of disease in both animals and humans. For example, identifying a genetic mutation in a particular immune pathway in affected Persian cats could reveal which components of immunity are most important for preventing dermatophyte infection. This, in turn, could be investigated in people and other animals and perhaps translated into improved genetic testing and therapies in a world where dermatophytes are becoming the nemesis of more than just Persian cats.

To this end, the aims of this dissertation research were designed to address the question: Why do Persian cats exhibit chronic and extensive dermatophytosis more often than other breeds of cat? The first aim and subject matter of Section 2 of this dissertation was to characterize the cutaneous microbiota of Persian cats with severe

dermatophytosis as compared to healthy Persian and non-Persian control cats. The host microbiome, as discussed in later sections, can serve as a defense mechanism against pathogens (Stacy and Belkaid 2019), and we hypothesized that alterations to the Persian cat microbiome could predispose these cats to severe dermatophytosis. The second aim and subject matter of Section 3 was to identify a genetic variant in Persian cats associated with severe dermatophytosis. We further sought to functionally validate and explain the evolutionary basis for a disease-associated allele containing AMP genes.

Before the research addressing these aims is presented in Sections 2 and 3, the remainder of this Introduction provides necessary background on dermatophytosis, the microbiome, and feline immunity and genetics.

1.2. Dermatophytosis in Humans and Animals

Dermatophytosis is an infection, typically of the hair, skin, and nails, caused by a group of keratinophilic fungi known as dermatophytes. Based on a study performed by the Global Burden of Disease Study 2013 Collaborators (2015), fungal skin disease lags behind only 6 other ailments in terms of worldwide prevalence: dental caries, headaches, age-related hearing loss, iron deficiency anemia, genital herpes, and ascariasis. Dermatophytosis is found worldwide, but the prevalence is higher in developing countries and areas with increased humidity (Bongomin et al. 2017). Though this disease is rarely fatal, its impact on human and animal welfare is enormous, exemplified by a large, ongoing epidemic of dermatophytosis in India thought to be due to abuse of

topical combined antifungal and steroid creams (Nenoff et al. 2019; Narang et al. 2019; Das et al. 2020; Patel et al. 2020).

Until quite recently, only three main genera of clinically important dermatophytes were described: *Trichophyton*, *Microsporum*, and *Epidermophyton* (Gnat et al. 2021). Recent molecular phylogenetic approaches have reorganized dermatophyte taxonomy and added six new genera: *Arthroderma*, *Ctenomyces*, *Guarromyces*, *Lophophyton*, *Nannizzia*, and *Paraphyton* (de Hoog et al. 2017). Different species of dermatophytes are adapted to different hosts and environments: anthropophilic species are adapted to live commensally on human hosts, zoophilic species on various animal hosts, and geophilic species in the environment (Table 1) (Moriello et al. 2017). Within the same genus, different species may have different host specificities; for example, *Trichophyton verrucosum* is zoophilic and adapted to the skin of cattle, while *Trichophyton rubrum* is anthropophilic and adapted to human hosts (Moriello et al. 2017). It appears that these fungi typically cause little inflammation in their usual reservoir host but tend to incite an acute inflammatory response when infecting a host for which they are not adapted (Weitzman and Summerbell 1995).

Table 1. Major dermatophytes of domestic animals and supposed reservoirs.

Dermatophyte	Main animal involved and reservoir(s)	Frequency in humans	Geographical distribution
Microsporum canis	Cats, dogs	Common	Worldwide
Trichophyton verrucosum	Cattle	Common	Worldwide
Trichophyton benhamiae (formerly *Arthroderma benhamiae*)	Guinea pigs	Common	Worldwide
Trichophyton erinacei	Hedgehogs	Occasional	Europe, East Asia, New Zealand
Trichophyton mentagrophytes (syn. *Arthroderma vanbreuseghemii*)	Cats, dogs, rabbits, rodents	Common	Worldwide
Trichophyton equinum	Horses	Occasional	Worldwide
Trichophyton simii	Monkeys, poultry, dogs	Rare	Rare outside of India
Lophophyton gallinae (formerly *Trichophyton gallinae*)	Chickens	Rare	Worldwide
Nannizzia persicolor (formerly *Microsporum persicolor*)	Rodents, voles	Rare	Europe, USA
Nannizzia nana (formerly *Microsporum nanum*)	Pigs	Rare	Worldwide
Trichophyton bullosum	Horses, donkeys	Rare	Tunisia, Sudan, Syria, France
Trichophyton quinckeanum	Mice	Rare	Worldwide
Nannizia gypsea (formerly *Microsporum gypseum*)	Soil (geophilic species)	Rare	Worldwide

NOTE.—Species names reflect the updated nomenclature presented by de Hoog et al. (2017), and traditional names are given in parentheses where applicable. Table adapted from Moriello et al. (2017).

Microsporum canis is a dermatophyte adapted to live on dogs and cats that is capable of causing zoonotic infections in humans (Moriello et al. 2017). Transmission to humans mainly occurs via contact with a cat, which may or may not show clinical signs of infection (Moriello et al. 2017; Gnat et al. 2018). Asymptomatic carriage of dermatophytes has been documented frequently in cats but only rarely in dogs (da Costa et al. 2013; Miller et al. 2013; Hnilica and Patterson 2017). Other terms besides asymptomatic carriage, such as "mechanical carriage" and "fomite carriage," are also used, reflecting uncertainty about the underlying mechanism for this carriage; it is unknown if the dermatophytes are actively adhering to or infiltrating the skin/hair (subclinical infection) or simply being passively carried on hairs.

Persian cats in particular are overrepresented when it comes to clinical dermatophytosis, and they tend to exhibit more chronic and extensive/generalized disease (Lewis et al. 1991; Moriello et al. 2017). Additionally, Persian cats may also be more predisposed to carry the disease asymptomatically. In one study performed in Brazilian catteries, 51/61 asymptomatic Persian cats were positive for *M. canis* via culture (Nitta et al. 2016). This is well above the proportion of cats typically reported as asymptomatic carriers (Nitta et al. 2016). Prevailing theories as to why Persians are more often and more severely affected than other breeds include 1) ineffective grooming of the long hair coat, 2) altered cutaneous microenvironment, or 3) a primary (genetic) immunodeficiency (Chang et al. 2011; Nuttall et al. 2008).

In both humans and animals, typical dermatophyte infection of the body involves hair loss with variable scaling, erythema, and pruritus, and the infection is typically

confined to one or a few focal areas (Merkhofer and Klein 2020; Miller et al. 2013). The lesion may be ring-shaped in humans, but ring shapes are uncommon in animals (Miller et al. 2013). These types of infection are mild and often self-limiting in both humans and animals (Merkhofer and Klein 2020; Miller et al. 2013). Rarely dermatophytosis may become severe (Rouzaud et al. 2015, 2018; Lanternier et al. 2013; Glocker et al. 2009). In these cases, the infection may become chronic, cover a large area of the body (extensive infection), and/or penetrate beyond the superficial keratin layer into the dermis. Extension of dermatophytosis into the dermis leads to the formation of visible nodules/masses in the skin. In human and veterinary medicine, these nodular forms of dermatophytosis are referred to by various names: Majocchi's granuloma, deep dermatophytosis, pseudomycetoma, mycetoma, and kerion (Durdu et al. 2020; Miller et al. 2013). Clinically, these forms all appear similar; histologically, there are subtle differences in the lesions (Durdu et al. 2020; Kano et al. 2009). Persian cats are well known for developing one of these types of nodular dermatophytosis: pseudomycetoma. Review of the literature found that of 35 reported cases of dermatophytic pseudomycetoma, 21 were Persian, 11 were of unknown breed, and 3 were non-Persian including 1 Maine Coon, 1 domestic longhair, and 1 domestic shorthair (Table 2) (Chang et al. 2011; Nuttall et al. 2008; Kano et al. 2009; Miller et al. 1986; Yager et al. 1986; Black et al. 2001; Bond et al. 2001; Zimmerman et al. 2003; Nardoni et al. 2007; Stanley et al. 2008; Ferro et al. 2008; Thian et al. 2008; Miller 2010; Nobre et al. 2010; Zafrany et al. 2014; Duangkaew et al. 2017; Bianchi et al. 2017).

Table 2. Literature review of feline pseudomycetoma cases as of March 2020.

Article	Breed	No. cases	Location of lesions	Diagnostics	Outcome	With classic lesions?
Miller 1986	Persian	1	NA	NA	NA	NA
Yager 1986	Persian	1	Skin (trunk)	Histology, culture	Euthanasia	YES
Black 2001	Persian	1	Intra-abdominal	Histology, IHC	Euthanasia	YES
Bond 2001	Persian	1	Skin (trunk, neck)	Histology, culture	Euthanasia	YES
Zimmerman 2003	Persian	1	Skin	Cytology, histology, culture	NA	YES
Nardoni 2007	NA	7	NA	NA	NA	NA
Nuttal 2008	Persian, Maine Coon	2	Skin (trunk, leg)	Cytology, histology, culture	Complete resolution	YES
Stanley 2008	Persian	1	Intra-pelvic	Histology, IHC	Euthanasia	NO
Ferro 2008	DSH	1	Intra-pelvic	Histology	NA	NA
Thian 2008	DLH	1	Skin (flank)	Histology, culture	Complete resolution	NO
Kano 2009	Persian	1	Skin (trunk)	Histology, cytology, culture, PCR	Complete resolution	NO
Miller 2010	Persian-4, NA-4	8	Skin (trunk-5, head-2, tail-1)	Histology	NA	2/8 cases
Nobre 2010	Persian	1	Skin (trunk, tail)	Histology, culture	Death	YES
Chang 2011	Persian	4	Skin (trunk, tail)	Histology, culture, PCR	2 resolved, 2 relapsed	YES
Zafrany 2014	Persian	1	Intra-pelvic	Histology, IHC	Complete resolution	YES
Duangkaew 2017	Persian	1	Skin (head, inguinal)	Histology, PCR	Death	YES
Bianchi 2017	Persian	2	Intra-abdominal	Histology	Euth, death	YES, NO

NOTE.—As indicated by the last column, not all cases of pseudomycetoma exhibit typical/classic lesions of dermatophytosis including hair loss, scaling, redness, etc. In some cases the lesions are confined to the deeper dermis and subcutaneous tissues with no change to the overlying skin and hair.

Only two cases of pseudomycetoma were found in dogs (Abramo et al. 2001). All feline and canine cases with definitive identification of the etiologic agent were caused by *M. canis*, while pseudomycetoma in humans has been reported to be caused by both *Microsporum* and *Trichophyton* spp.

1.3. Pathogenesis of Dermatophytosis

Infection is initiated when the infective form of the fungus, the arthrospore (alternately referred to as arthroconidium, conidium, or simply 'spore'), adheres to host corneocytes at the skin surface (Moriello et al. 2017). Arthrospores are small segments that break off from fungal hyphae (Figure 1) and that can maintain viability for months to years in the environment. They can be transmitted from animal to animal, from environment to animal, or from fomite (such as bedding, grooming tools, ectoparasites) to animal. Adherence of arthrospores to corneocytes is reported to take 2-6 hours and is thought to be mediated by fungal adhesins and proteases such as keratinases and subtilisins (Baldo et al. 2010, 2011). The exact mechanism by which these proteases facilitate adherence is not yet understood. The pattern of protease expression by dermatophytes is thought to be species or host-specific and may influence the degree of host inflammation and immune response (Moriello et al. 2017). During adherence, arthrospores of at least some species of dermatophytes send out fibrils that attach and anchor the spores to the stratum corneum (Baldo et al. 2011). It appears that grooming of cats may be a host defense mechanism against adherence, as *M. canis* infection could not be experimentally established in one colony of cats until grooming was restricted

(DeBoer and Moriello 1994). Additionally, spore adherence only occurred readily when the skin was lightly abraded and kept moist (DeBoer and Moriello 1994).

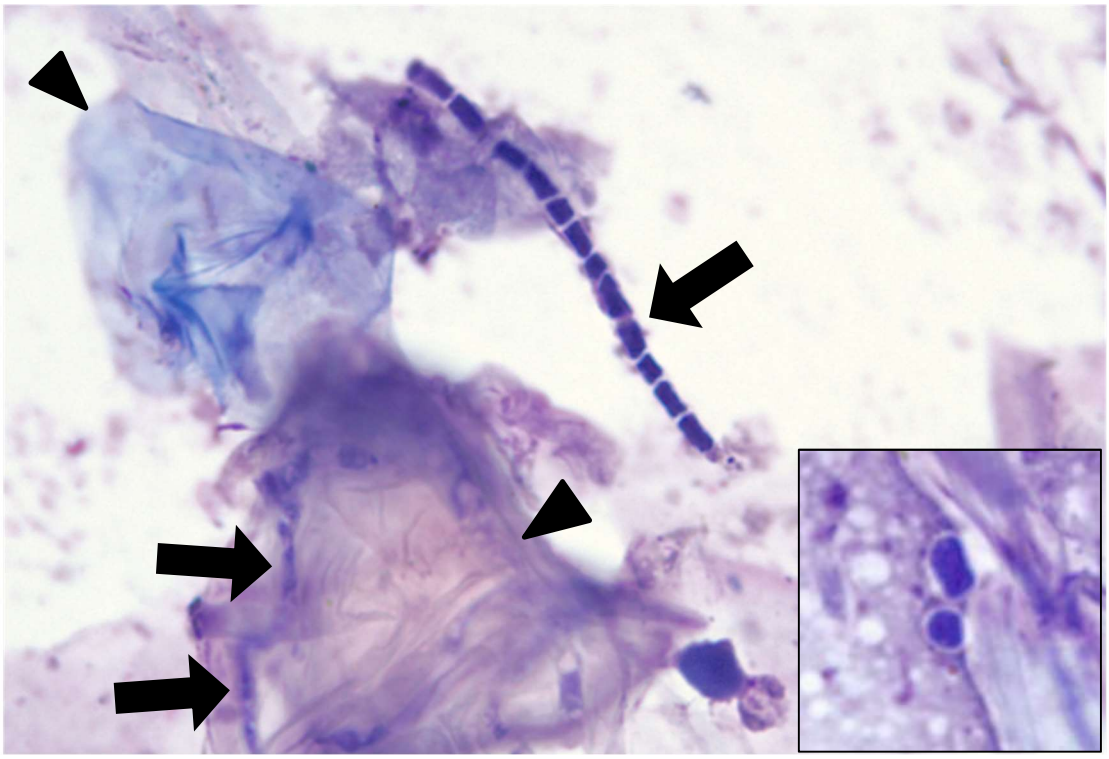

Figure 1. Photomicrograph of skin scraped from a dog with PCR/sequencing-confirmed dermatophytosis (*Trichophyton mentagrophytes* infection).
Fungal hyphae (black arrows) are intermingled with canine corneocytes (black arrowheads). The hyphal segments will break off as the hyphae matures to become infective arthrospores. Inset: Two arthrospores after breaking off from hyphae. Diff-Quik stain. 1000x magnification.

Following adhesion of an arthrospore to the skin surface, invasion of the epithelium occurs as the arthrospore begins to germinate (Baldo et al. 2011). The arthrospore sends germ tubes through the corneocytes longitudinally and perpendicularly (Aljabre et al. 1992). Germ tubes mature into hyphae which continue invading into

keratinized structures including hair follicles, hair, and nails (Figure 2). Eventually, hyphae will fully mature and shed new arthroconidia in approximately 7 days, completing the life cycle of the fungus (Aljabre et al. 1992). Infected hairs and skin cells are lost into the environment, serving as a source of infection for others. Numerous host immune mechanisms have been identified to combat dermatophyte invasion, and these are described further in section 1.5.

Figure 2. Photomicrograph of a histologic section of feline skin.
In the center of the image is a hair follicle containing a hair shaft (black arrow), which is invaded by and surrounded by *Microsporum canis* hyphae and arthrospores (black arrowhead). H&E stain. 200x magnification.

1.4. The Cutaneous Microbiome and its Relevance to Dermatophytosis

Collectively, the microbes that inhabit epithelial surfaces of humans and animals are known as microbiota and compose the microbiome. The microbiome, particularly of the gut but also the skin, has become a source of intense investigation in recent years given the myriad roles it plays in health and disease, including 1) priming of the host immune system, 2) prevention of infection with pathogens, and 3) secretion of metabolites important for host health (Grice and Segre 2011; Gallo and Nakatsuji 2011; Stacy and Belkaid 2019). NGS has allowed for more in depth examination of the microbiome than classical methods such as culture (Grice and Segre 2011).

NGS studies of the cutaneous microbiome, including both shotgun metagenomic and amplicon sequencing studies, have revealed an amazing variety of microbes on the skin surface and have shown that disruption of microbial communities (dysbiosis) is associated with a variety of diseases/processes: atopic dermatitis, acne vulgaris, psoriasis, wound healing, cutaneous malignancies, white-nose syndrome in bats, systemic lupus erythematosus, and others (Sander et al. 2019; Grisnik et al. 2020; Meason-Smith et al. 2016; Langan et al. 2019). Most studies of the microbiome in disease are descriptive in nature and do not yet address questions of causation. It is often difficult to determine whether dysbiosis led to the disease in question or whether it is a product of the disease state (Sander et al. 2019). However, some studies, particularly of the gut microbiome, do support a causal role of the microbiota in disease such as one study showing that the host phenotype (e.g., obesity) can be transferred via microbiota transfer (Koh et al. 2020). In this age of descriptive microbiome studies with uncertain

causation, alterations of microbiota and associated microbial metabolites can still shed light on mechanisms of disease, serve as a biomarker for diagnostic assays, or represent a therapeutic target.

Importantly, the microbiome has been found to protect against colonization by other pathogens by competing for essential nutrients, inducing host immune responses, and producing AMPs (Kamada et al. 2013; Gallo and Nakatsuji 2011; Stacy and Belkaid 2019). Particular members of the cutaneous microbiota, including *Staphylococcus epidermidis*, were shown to activate components of host adaptive immunity including particular T-cell subsets (Stacy and Belkaid 2019). *S. epidermidis* in particular, can recruit cytotoxic T-cells to the skin that can induce host AMP production for protection against pathogens (Stacy and Belkaid 2019). *S. epidermidis* can also directly harm pathogens by secreting its own AMPs and proteases or competing for nutrients (Stacy and Belkaid 2019). This role of the microbiome could be important in protecting against dermatophyte infection.

The microbiomes of both dogs and cats have been characterized using amplicon-based sequencing, including the bacterial microbiome (16S amplicon-sequencing) and the fungal "mycobiome" (ITS amplicon-sequencing) (Meason-Smith et al. 2015, 2016; Older et al. 2019). In cats, breed and indoor versus outdoor lifestyle were evaluated and found to affect the microbiome, suggesting that these factors should be controlled for during experimental design (Older et al. 2019). Hair coat length was shown to have a potentially mild effect (Older et al. 2019). In one study, a Sphynx cat with no clinical signs of dermatophytosis was found to harbor *Microsporum* sp. on its back (0.08%

relative abundance, per discussion with study authors), suggestive of asymptomatic carriage (Older et al. 2019). In another study, only one cat, a Persian, was identified with high relative abundance of *Microsporum* sp. in the groin region (Meason-Smith et al. 2016). The cat had clinically recovered from a bout of dermatophytosis a few months prior to participation in the study (per discussion with study authors) and had no lesions at the time of sampling, again suggestive of asymptomatic carriage of dermatophytes. Approximately one month following sample collection, this cat was found to have relapsed with active lesions of dermatophytosis. These findings demonstrate the ability of NGS to detect potential asymptomatic carrier cats.

1.5. Dermatophytosis: Immunity and Genetics

Both the innate and adaptive immune responses play a role in antifungal immunity, and genetic alterations in immune genes have been reported in association with dermatophytosis (Table 3) (Rouzaud et al. 2015; Lanternier et al. 2013; Glocker et al. 2009; Nielsen et al. 2015; Ferwerda et al. 2009; Jaradat et al. 2015; Abdel-Rahman and Preuett 2012; Sadahiro et al. 2004; Asz-Sigall et al. 2010; Garcia-Romero et al. 2012). The first thing a cutaneous fungal pathogen such as a dermatophyte encounters when it begins its invasion is the intact skin barrier, the first blockade of the innate immune system. This physical barrier, along with its associated skin-surface AMPs and host microbiome, work to repel the invader (Gallo and Nakatsuji 2011; Smeekens et al. 2014; Drummond et al. 2014; Fritz et al. 2012). Based on the current understanding of dermatophyte pathogenesis, the fungus will take advantage of microtrauma in the skin to

begin adhering to and penetrating corneocytes (Moriello et al. 2017). The dermatophyte can, at this point, activate receptors on the surface of myeloid cells or keratinocytes known as pathogen recognition receptors (PRRs); critical PRRs for antifungal defense include the C-type lectin receptors (CLRs) such as DECTIN-1 and DECTIN-2 and, to a lesser extent, toll-like receptors (TLRs), TLR-2 and TLR-4 (Drummond et al. 2014; Garcia-Romero et al. 2015). Specifically, these PRRs recognize molecules such as β-glucans on the surface of the fungi. Only one genetic variant in PRRs has been associated with fungal disease, and this variant in the gene encoding DECTIN-1 (CLEC7A) has been only tenuously associated with nail dermatophytosis in humans (Ferwerda et al. 2009; Marodi and Erdos 2010). Variants in individual PRR genes are thought to be less likely to cause disease due to the redundancy and collaborative responses across PRR receptors (Drummond et al. 2014).

Activation of several different CLRs initiates intracellular signaling through the well-described CARD9 pathway. This pathway, involving SYK kinase, CARD9, BCL10, and MALT1, culminates in activation of NF-κB and ERK to induce pro-inflammatory cytokine production, including the critical antifungal cytokine IL-17 (Drummond et al. 2016). *Card9*-/- mice completely lose the ability to defend against systemic fungal infections and experience 100% mortality (Corvilain et al. 2018). In humans, *CARD9* is the only gene associated with invasive/deep fungal infections (Merkhofer and Klein 2020). Several different autosomal recessive, nonsense and missense *CARD9* mutations have now been identified in humans from the USA, Canada, Europe, Middle East, South America, and China and are associated with extensive

and/or deep dermatophytosis caused by *Trichophyton* spp.; other types of fungal infections (candidiasis, phaeohyphomycosis) are seen in some cases (Drummond et al. 2016; Vaezi et al. 2018). At this point, it is still unclear why CARD9 deficiency is associated primarily with dermatophytosis over other fungal infections and why some patients live for decades before developing severe fungal infections while others develop disease early in life (Drummond et al. 2016).

The innate recognition of fungi and induction of the CARD9 pathway leads to induction of adaptive, cell-mediated immunity and the Th17 response, which appears necessary for controlling superficial fungal skin infections (Sparber et al. 2018; Burstein et al. 2018). In a recently developed mouse model of *M. canis* infection, mice deficient in IL-17 or its receptors showed more extensive colonization of the epidermis and a stronger, more inflammatory Th1 response (Burstein et al. 2018). No invasion beyond the epidermis was noted in the IL-17 deficient mice (Burstein et al. 2018). In the very small number of human cases of IL-17 primary immunodeficiency, an increased prevalence of dermatophytosis has not been reported (Sparber et al. 2018).

It is reported that IL-17 increases the expression of antifungal AMPs at the skin surface, including human β-defensin 2 and S100A7/psoriasin (Burstein et al. 2018). An immunohistochemical study of skin in adult T-cell leukemia/lymphoma patients (highly predisposed to dermatophytosis) found that IL-17 producing cells and S100A7 expression were markedly reduced in affected patients versus healthy controls (Sawada et al. 2013). S100A7 has been shown to exhibit strong anti-dermatophyte activity *in vitro* and is highly expressed in normal cases of human dermatophytosis (Fritz et al. 2012).

In one additional immunohistochemical study, CD1a+ Langerhans cells were found to be present in lower numbers in the affected and unaffected epidermis of human patients with dermatophytosis versus healthy controls (Reis et al. 2019). Langerhans cells are important dendritic cells found in the epidermis that surveille for pathogens and sample pathogens for presentation to the adaptive immune system. The authors postulate having low numbers of these cells in the epidermis could be a risk factor for dermatophytosis but cautioned that additional study is needed (Reis et al. 2019).

Regarding the genetics of dermatophytosis, it is also important to note that an early study identified an autosomal recessive mode of inheritance for susceptibility to chronic infection with the dermatophyte *Trichophyton concentricum* (Serjeantson and Lawrence 1977). However, other researchers found an autosomal dominant mode of inheritance for this phenotype, and others were unable to identify a pattern of inheritance (Abdel-Rahman 2017). The findings were controversial, and a specific genetic locus associated with disease was never identified in the affected populations.

Table 3. Literature review of genetics of dermatophytosis.
Initial studies for each gene.

Article	Genetics of what aspect?	Genotyping method	Approach to genetic mapping	Genes implicated	Type of variant	Notes
Glocker 2009	Severe CMC and chronic dermatophytosis	SNP array	Linkage analysis; candidate gene	*CARD9*	SNV (nonsense), AR	Q295X; Iranian family; validated
Lanternier 2013	Severe, chronic and deep dermatophytosis	Sanger sequencing	Candidate gene	*CARD9*	SNV (nonsense), AR	Q289X; African families; validated; *Trichophyton* spp.
Nielsen 2015	CMC,bacterial abscesses, extensive dermatophytosis	Exome sequencing	Candidate gene	*STAT1*	SNV (missense), AD	*T. mentagrophytes*; gain-of-function mutation; validated
Ferwerda 2009	CMC and nail dermatophytosis	Sanger sequencing	Candidate gene	*CLEC7A* (Dectin-1)	SNV (nonsense)	Not validated; controversial; Y238X
Jaradat 2015	Susceptibility to typical dermatophytosis	qPCR	Candidate gene	*DEFB4*	CNV	Not validated
Abdel-Rahman 2012	Susceptibility to typical dermatophytosis	SNP array	GWAS; candidate gene	21 genes	SNVs	Not validated; small sample size
Sadahiro 2004	Chronic dermatophytosis	HLA typing kits	Candidate gene	HLA genes	NA	Not validated
Asz-Sigall 2010	Susceptibility to nail dermatophytosis	HLA typing	Candidate gene	HLA genes	NA	Not validated

NOTE.—AD, autosomal dominant; AR, autosomal recessive; CMC, chronic mucocutaneous candidiasis; CNV, copy number variant.

1.6. Feline Genetic Diseases and Approaches

The desire to improve the health of cats and their utility as animal models has led to rapid advances in feline genomics and the development of a consortium dedicated to uncovering cat genetic variation (the 99 Lives Cat Genome Sequencing Initiative) (Lyons 2019). Several tools for investigating the genetics of feline diseases are now available to veterinarians and researchers, including NGS technologies, a high-quality feline genome assembly (felCat9), and a growing database of feline genomic variation curated by the 99Lives Consortium (Lyons 2019; Li et al. 2016; Mauler et al. 2017). Approximately twenty examples now exist of feline genetic diseases or traits that have

been elucidated using whole genome sequencing in conjunction with bioinformatic and statistical analyses (Lyons 2019). Examples of genetic diseases that have been investigated in client-owned cats using whole-genome sequencing include neurodegenerative disease (Niemann-Pick type C1), cardiac disease (hypertrophic cardiomyopathy), hematologic disease (cytochrome b5 reductase deficiency), ocular diseases (retinopathies and cataracts), and others (Mauler et al. 2017; Ontiveros et al. 2019; Oh et al. 2017; Jaffey et al. 2019).

For rare Mendelian diseases, likely causative mutations have been found by analyzing DNA from a single animal or few affected animals in conjunction with the 99Lives database of genomic variation (Mauler et al. 2017). This approach identifies variants that are unique to the animal with the disease/trait of interest and not present in a large number of control animals. As many variants will be identified by this approach that are not pathogenic, disease-causing variants must be narrowed down by examining evolutionary conservation, potential effects on protein structure, population allele frequencies, and functional genomics data, where available (Eilbeck et al. 2017).

For diseases where populations of cases and controls can be sampled, GWAS studies allow for identification of SNPs that are significantly associated with disease. GWAS using linear mixed models (for example, EMMAX) has become popular for its ability to correct for population structure and relatedness (Zhou and Stephens 2012). GWAS can be performed with smaller sample sizes in dogs and cats than in humans due to higher linkage disequilibrium (Karlsson et al. 2007; Gandolfi et al. 2018). GWAS for monogenic traits or large effect variants also requires fewer samples than GWAS for

polygenic traits. When causative mutations are identified, diagnostic tests can be developed and targeted treatments sought, improving overall patient care. Modern NGS technologies coupled with continually improving genome assemblies allow for identification of disease variants which can provide a deeper understanding of disease pathogenesis in cats.

2. CHARACTERIZATION OF THE CUTANEOUS MYCOBIOTA IN PERSIAN CATS WITH SEVERE DERMATOPHYTOSIS*

2.1. Introduction

Dermatophytosis is a common infection of the hair, skin, and nails caused by a group of keratinophilic, filamentous fungi referred to as dermatophytes (Gnat et al. 2019). This disease occurs in humans and animals worldwide, and is caused by several different species of dermatophytes that exhibit preferences for particular hosts (Gnat et al. 2019). While dermatophytosis is typically mild and self-limiting, it is a zoonotic disease with an enormous impact on human and animal welfare (Gnat et al. 2019). Though uncommon, severe infections, including deep, nodular infections, are reported in both humans and animals (Lanternier et al. 2013; Chang et al. 2011).

Feline dermatophytosis is most commonly caused by *Microsporum canis* (Moriello et al. 2017). In one study, Persian cats represented 5% of the total cats seen by a small animal hospital but accounted for 25% of the cats diagnosed with dermatophytosis (Lewis et al. 1991). Additionally, dermatophytic pseudomycetomas (pyogranulomatous masses caused by the fungus) occur almost exclusively in Persian cats (Moriello et al. 2017). It has been suggested that asymptomatic carriage of dermatophytes (also referred to as “mechanical carriage” of spores or “fomite carriage”)

*Reprinted with permission from "Characterization of the cutaneous mycobiota in Persian cats with severe dermatophytosis" by Alexandra N. Myers, Caitlin E. Older, Alison B. Diesel, Sara D. Lawhon, Aline Rodrigues Hoffmann, 2021, Veterinary Dermatology, Copyright 2021 ESVD and ACVD.

is more common in Persian cats than in other breeds (Nitta et al. 2016); however, this has not been thoroughly investigated outside of contaminated catteries.

It is unknown why Persian cats are afflicted more commonly and more severely than other breeds. Prevailing theories include 1) ineffective grooming of the long hair coat, 2) an altered cutaneous microenvironment, or 3) a primary (genetic) immunodeficiency (Nuttall et al. 2008). A recent study of feline grooming mechanics provides some support for ineffective grooming in Persian cats (Noel and Hu 2018). Only anecdotal evidence exists thus far for a potential genetic predisposition. Alterations to the feline cutaneous microenvironment during dermatophytosis, particularly alterations in the microbiota, have only been examined with culture-based methods. In one particular culture-based study, cats initially infected with *M. canis* had cultures with mixed populations of *M. canis* and saprophytic fungi; after 30 days, all of these cats had pure cultures of *M. canis*, suggesting decreased fungal diversity in the face of clinical dermatophytosis (Moriello 1991).

NGS methods have allowed for more in-depth examination of the cutaneous microbiome than culture-based methods and have revealed a wide variety of microbes on the skin surface (Findley et al. 2013). Several NGS studies have shown that disruption of microbial communities (dysbiosis) is associated with a variety of diseases/processes in humans and animals, including atopic dermatitis, acne vulgaris, psoriasis, wound healing, cutaneous malignancies, and white-nose syndrome in bats (Sander et al. 2019; Grisnik et al. 2020; Meason-Smith et al. 2016; Langan et al. 2019).

Importantly, the microbiome has been found to protect against colonization by pathogens. For example, particular members of the cutaneous microbiota, including *Staphylococcus epidermidis*, were shown to activate components of host adaptive immunity including particular T-cell subsets (Stacy and Belkaid 2019). *S. epidermidis* can also directly harm pathogens by secreting AMPs and proteases or competing for nutrients (Stacy and Belkaid 2019). Therefore, the bacterial and fungal cutaneous microbiota could be important in protecting the host against dermatophyte infection.

In this study, we employed targeted next-generation sequencing and quantitative PCR to profile the fungal microbiome of Persian cats with severe dermatophytosis. We hypothesized that Persian cats with severe disease would exhibit a cutaneous dysbiosis characterized by decreased microbial diversity and a high relative abundance of *Microsporum canis*. We further hypothesized that healthy Persian cats would harbor different microbial populations than non-Persian cats.

2.2. Materials and Methods

2.2.1. Ethics

An animal use protocol (IACUC 2018-0256 CA) was approved by the Texas A&M University Institutional Animal Care and Use Committee to enroll clinical cases for this study. Informed written consent was obtained from each owner.

2.2.2. Participants

Study participants included 26 adult Persian cats and 10 adult domestic long-haired cats (Table 1). Detailed sample metadata can be found in Appendix A. Persian cats were divided into three groups according to their clinical history and veterinary exam findings. Group 1, referred to as 'naïve Persian controls', included 11 Persian cats with no lesions or history of dermatophytosis; Group 2, referred to as 'resistant Persian controls', included eight Persian cats with documented past exposure to dermatophytes but no history of severe/chronic infection; Group 3, referred to as 'Persian cases', included seven Persian cats with severe infections, including disseminated, chronic, and deep infections (cases). Ten healthy DLH cats with no history of dermatophytosis served as a non-breed matched control population.

All Group 3 cats had at least two different diagnostic tests positive for dermatophytosis at the time of sample collection, including culture and one or more of the following: Wood's lamp examination, skin cytology, trichogram, PCR, or biopsy. These cats exhibited clinical signs including alopecia over a large area of the body, scaling, erythema, pruritus, and easily epilated hair. Five of these cats had chronic or recurrent infections despite previous treatment with oral itraconazole or terbinafine and topical lime sulfur treatments. Two cats had biopsy-confirmed pseudomycetoma in addition to the lesions previously described. Three of the Persian cases received oral and/or topical antifungal treatment within one month of sample collection.

2.2.3. Sample Collection and Sequencing

For each animal, two skin swabs (Isohelix, Cell Projects Ltd., Harrietsham, UK) were rubbed on five total skin sites: inter-scapular, dorsal tail-base, axilla, groin, and facial folds. These two swabs were immediately stored together in a single MoBio PowerBead tube (MoBio Laboratories, Inc., CA, USA), and this sample was referred to as the 'general' swab. For each of six Group 3 Persian cats with lesions, two additional swabs were rubbed on a single lesion. These two swabs were immediately stored together in a single MoBio PowerBead tube, and this sample was referred to as the 'lesion' swab. During swabbing, the hair was spread with gloved hands and swabs were rubbed ten times on each side of the swab on the skin within a 1 in^2 area at each site. All swabs were stored within the MoBio PowerBead tube at 4°C for no more than two weeks before DNA extraction. Owners were instructed to use the same swabbing method—using the same type of swab—to collect samples from the household environment (specifically a site of carpet or bedding frequented by the cat).

DNA was extracted from skin and household environmental swabs using the MoBio PowerSoil® DNA Isolation Kit (MoBio Laboratories, Inc., CA, USA) with a modified protocol. Modifications to the manufacturer's protocol were 1) a reduction in volume of Solution C4 from 1.2 mL to 900 µL and 2) a reduction in volume of Solution C6 from 100 µL to 50 µL. Negative extraction controls were performed, including an unused Isohelix swab and a MoBio PowerBead tube without a swab. 16S sequencing was not performed on the environmental swabs.

Extracted DNA was sequenced at the University of Minnesota Genomics Center (Minneapolis, MN, USA) on an Illumina MiSeq (Illumina, Inc., San Diego, CA). The fungal ITS1 region was targeted using primers forward ITS1F_Nextera: TCGTCGGCAGCGTCAGATGTGTATAAGAGACAGCTTGGTCATTTAGAGGAAG TAA and reverse ITS2_Nextera: GTCTCGTGGGCTCGGAGATGTGTATAAGAGACAGGCTGCGTTCTTCATCGAT GC. The 16S V1-V3 region was targeted using primers V1_27F_Nextera: TCGTCGGCAGCGTCAGATGTGTATAAGAGACAGAGAGTTTGATCMTGGCTC AG and V3_534R_Nextera: GTCTCGTGGGCTCGGAGATGTGTATAAGAGACAGATTACCGCGGCTGCTGG. Due to the low number of bacterial reads in many of these samples and lack of amplification of *Staphylococcus* spp. from the mock community (positive control), the results of the 16S microbiota analysis were minimally interpreted. The sequences analyzed are available in the NCBI Sequence Read Archive under BioProject ID PRJNA704990.

qPCR targeting the ITS1 region was performed as described in section 1A.II of the protocol developed by Gohl et al (2016). The qPCR was performed for 35 cycles on undiluted as well as 8-fold and 64-fold diluted template using the same primers as above. The resulting Cq values provided an estimate of the absolute abundance of fungal DNA in each sample.

2.2.4. Data Analysis

Raw ITS and 16S sequencing data were adapter- and quality-trimmed using Trim Galore! (https://www.bioinformatics.babraham.ac.uk/projects/trim_galore/). Quality trimming was performed to a quality threshold of 18 as recommended by Mohsen et al (2019). ITS sequences were further processed with QIIME 2 v.2020.2 (Bolyen et al. 2019), including denoising with DADA2 (Callahan et al. 2016) and taxonomy assignment using the UNITE (dynamic_04.02.2020) ITS database for fungi (Nilsson et al. 2018) and a scikit-learn classifier (Abraham et al. 2014). For bacteria, the SILVA 16S v132 99% database was used for taxonomy assignment (Quast et al. 2012).

Removal of contaminant taxa was performed for both ITS and 16S sequencing data. For ITS data, the Decontam R package (Davis et al. 2018) was used to remove two contaminant taxa using the "prevalence" method with the isContaminant command at a probability threshold of 0.5. Manual filtering was performed for one particular amplicon sequence variant (correlating with *Malassezia* sp.) that was not removed by Decontam but was highly abundant in the swab control sample. For 16S data, The Decontam R package was used to remove contaminant taxa using the "prevalence" method and the isNotContaminant command. ASVs attributed to *Methylobacterium* spp., a previously described contaminant in microbiota studies (Salter et al. 2014), were also removed, in addition to sequences not classified to at least phylum-level.

Alpha diversity metrics including Shannon, Pielou's evenness, and observed ASVs were calculated to uncover species richness and evenness within samples. Faith's phylogenetic diversity was also calculated for 16S data. Distance matrices were

generated using Bray-Curtis dissimilarity and Jaccard distance metrics to enable evaluation of community structure and were visualized using PCoA plots generated with Emperor (Vazquez-Baeza et al. 2013, 2017). Weighted and unweighted UniFrac metrics were also used for bacterial 16S data.

2.2.5. Dermatophyte Culture

Toothbrushes were used to collect hair samples and to inoculate DTM plates (Hardy Diagnostics, Santa Maria, CA, USA) using the Mackenzie toothbrush method (Moriello et al. 2017). Plates were incubated at room temperature and evaluated daily for fungal growth for up to 21 days. If a potential dermatophyte could not be definitively identified by standard morphological methods, direct colony PCR targeting the fungal ITS2 region was performed followed by Sanger sequencing to confirm the identity of the colony (see section 2.2.6). The number of dermatophyte colonies was used to help differentiate asymptomatic/fomite carriers and infected individuals, as previously described (Moriello et al. 2017).

2.2.6. Direct colony PCR

If a potential dermatophyte could not be definitively identified by standard morphological methods, direct colony PCR targeting the fungal ITS2 region was performed followed by Sanger sequencing to confirm the identity of the colony. Sequencing of the fungal ITS2 region allows for differentiation of *Microsporum canis* from other dermatophyte species (Li et al. 2008).

As described by Walch et al. (2016), a pinpoint amount of the fungal colony in question was collected with a sterile, disposable inoculation needle and placed directly into the PCR reaction mixture described below.

Conventional PCR targeting the fungal ITS2 region was performed with the following primers: ITS3-F (5'-GCATCGATGAAGAACGCAGC-3') and ITS4-R (5'-TCCTCCGCTTATTGATATGC-3'). The total volume of the PCR reaction was 25 µL consisting of 12.5 µL of AccuStart II PCR ToughMix (Quantabio, Beverly, MA, USA) 0.2 µM of each primer, 1 µL of template or pinpoint amount of fungal colony, and water up to the reaction volume. The reaction mixture was denatured at 95°C for 3 min, followed by 40 cycles of denaturation at 95°C for 15 s, annealing at 59°C for 15 s, and extension at 68°C for 45 s. This was followed by a final extension step for 5 min at 68°C in a T100TM Thermal cycler (Bio-RAD Laboratories, Emeryville, CA, USA). Each batch of PCRs included a negative PCR control (template consisting of 1 µL of DNA-free molecular-biology-grade water), and a positive PCR control (1 µL of purified *Cryptococcus neoformans* DNA).

PCR products were submitted to a commercial laboratory (Eton Bioscience, Inc., San Diego, CA, USA) for purification and Sanger sequencing. Sequences were queried with BLASTn (National Center of Biotechnology Information, Washington DC, www.ncbi.nlm.nih.gov/BLAST).

2.2.7. Statistical Methods

Statistical significance of qPCR results and alpha diversity results was analyzed using the Wilcoxon rank sum or Kruskal-Wallis test in JMP Pro 15 (SAS Institute, Cary, NC, USA). For beta diversity results, ANOSIM (analysis of similarities) was performed on the distance matrices using the vegan package in R (Oksanen et al. 2019). Linear Discriminant Analysis (LDA) Effect Size (LEfSe) algorithm (Segata et al. 2011) was used to analyze differential taxa abundance with an LDA cutoff score of 2.5 and significance cutoff of $p<0.01$. The Benjamini-Hochberg procedure for p-value correction (Benjamini and Hochberg 1995) was used to correct for multiple comparisons where appropriate.

2.3. Results

For NGS targeting the ITS region, 55 samples were collected from Group 1, Group 2, and DLH healthy control cats (29 general swabs and 11 environment swabs) and Group 3 Persian cats with severe dermatophytosis (7 general swabs, 6 lesion swabs, and 2 environment swabs; Table 4). Of these samples, three were excluded from downstream analysis due to low sequence counts: One severe dermatophytosis general swab (sample 30G) and two healthy DLH general swabs (samples 23G and 26G).

After filtering, 1,018 ASVs were identified from four fungal phyla: *Ascomycota*, *Basidiomycota*, *Chytridiomycota*, and *Mucoromycota*. The mean number of reads per sample was 10,648. The feature table was rarefied to 1,800 sequences/sample.

Table 4. Overview of cats enrolled in cutaneous microbiota study.

Cat#	Group	Samples Collected	Age	Sex	Recent Antifungals
1	naïve Persian control	G, E	1-5	M	no
2	naïve Persian control	G, E	>10	F	no
3	naïve Persian control	G	>10	F	no
4	naïve Persian control	G, E	6-10	M	no
5	naïve Persian control	G	1-5	M	no
6	naïve Persian control	G, E	1-5	F	no
7	naïve Persian control	G, E	>10	M	no
8	naïve Persian control	G, E	>10	M	no
9	naïve Persian control	G	1-5	M	no
10	naïve Persian control	G, E	>10	F	no
11	naïve Persian control	G, E	>10	F	no
12	resistant Persian control	G	>10	M	no
13	resistant Persian control	G	>10	M	no
14	resistant Persian control	G, E	1-5	F	no
15	resistant Persian control	G	6-10	M	no
16	resistant Persian control	G	6-10	F	no
17	resistant Persian control	G	6-10	F	no
18	resistant Persian control	G, E	1-5	M	no
19	resistant Persian control	G, E	6-10	M	no
20	DLH control	G	1-5	F	no
21	DLH control	G	1-5	F	no
22	DLH control	G	6-10	M	no
23	DLH control	G	>10	F	no
24	DLH control	G	>10	F	no
25	DLH control	G	1-5	M	no
26	DLH control	G	1-5	M	no
27	DLH control	G	6-10	M	no
28	DLH control	G	>10	F	no
29	DLH control	G	1-5	M	no
30	Persian case	G, L, E	>10	M	no
31	Persian case	G, L	6-10	F	no
32	Persian case	G, L	1-5	F	yes
33	Persian case	G, L	6-10	F	no
34	Persian case	G, L	6-10	M	no
35	Persian case	G	1-5	F	yes
36	Persian case	G, L, E	6-10	M	yes

NOTE.—DLH, domestic longhair; E, environmental swab; F, female; G, general swab; L, lesion swab; M, male. Reprinted with permission from Myers et al. (2021).

For NGS targeting the 16S V1-V3 region, 42 samples were collected and sequenced (same samples used for ITS sequencing, minus the environmental swabs) in addition to negative control swabs and a mock community (positive control) swab. Detailed sample metadata can be found in Appendix A. Of these samples, 14 were excluded from downstream analysis due to low sequence counts, leaving 8 DLH control swabs, 15 Persian control swabs, and 5 Persian severe dermatophytosis swabs (including both general and lesion swabs). The mean number of 16S reads per sample was 7,207. The feature table was rarefied to 1,500 sequences/sample. The bacterial mock community submitted as a positive control sample had a theoretical/expected relative abundance of *Staphylococcus* spp. of 24%. After data processing, the mock sample was found to have only 0.37% relative abundance of *Staphylococcus* spp. while all other taxa exhibited relative abundances that were similar to expected.

2.3.1. Species richness and diversity

For fungi, alpha diversity metrics (Shannon, observed ASVs, and Pielou's evenness) showed no significant differences in fungal species evenness or richness between healthy Persian cats and healthy DLH cats or between Persian cats with dermatophytosis and all healthy cats (Table 5). Likewise, no differences were observed between lesion swabs and the general swabs collected from the same affected cats (Shannon p=0.505; Observed ASVs p=0.360; Pielou's p=0.627).

For bacterial alpha diversity metrics, no significant differences were observed between Persians with dermatophytosis and all healthy cats or between healthy Persian cats and healthy DLH cats (Table 6).

Table 5. Statistical analysis of fungal alpha and beta diversity metrics.

	Cases (General + Lesion Swabs) vs All Control	Lesion Swabs Only vs All Control	Healthy Persian vs DLH
Alpha Diversity			
Observed ASVs	0.763	0.726	0.625
Shannon	0.505	0.926	0.926
Pielou's	0.342	0.898	0.912
Beta Diversity			
Bray Curtis	**R=0.14, p=0.05**	**R=0.22, p=0.05**	R=-0.05, p=0.84
Jaccard	R=0.14, p=0.06	R=0.23, p=0.06	R=-0.07, p=0.87

NOTE.—All alpha diversity values are Wilcoxon rank sum p-values. Beta diversity values are ANOSIM R values and p-values. Bolded values are significant at p=0.05 or less. Reprinted with permission from Myers et al. (2021).

2.3.2. Microbial community structure

Fungal community structure (beta diversity) was mildly but significantly different between all healthy cats and Persian cats with dermatophytosis, as demonstrated by the Bray-Curtis dissimilarity index (Figure 3 and Table 5). However, the Jaccard distance metric did not indicate significance (Table 5). No differences in fungal community structure were observed between healthy Persian cats and healthy DLH cats (Table 5).

For bacterial beta diversity metrics, no significant differences were observed between Persians with dermatophytosis and all healthy cats or between healthy Persian cats and healthy DLH cats (Table 6).

Table 6. Statistical analysis of bacterial alpha and beta diversity metrics.

	Case (General + Lesion Swabs) vs All Control	Healthy Persian vs DLH
Alpha Diversity		
Observed ASVs	0.4288	0.4288
Shannon	0.2411	0.2411
Pielou's evenness	0.7415	0.7026
Faith's PD	0.4894	0.4894
Beta Diversity		
Bray Curtis	R=0.05, p=0.75	R=-0.04, p=0.75
Jaccard	R=0.04, p=0.34	R=0.09, p=0.34
Unweighted UniFrac	R=0, p=0.45	R=-0.01, p=0.45
Weighted UniFrac	R=0, p=0.45	R=0.07, p=0.31

NOTE.—All alpha diversity values are Wilcoxon rank sum p-values. Beta diversity values are ANOSIM R values and p-values. Reprinted with permission from Myers et al. (2021).

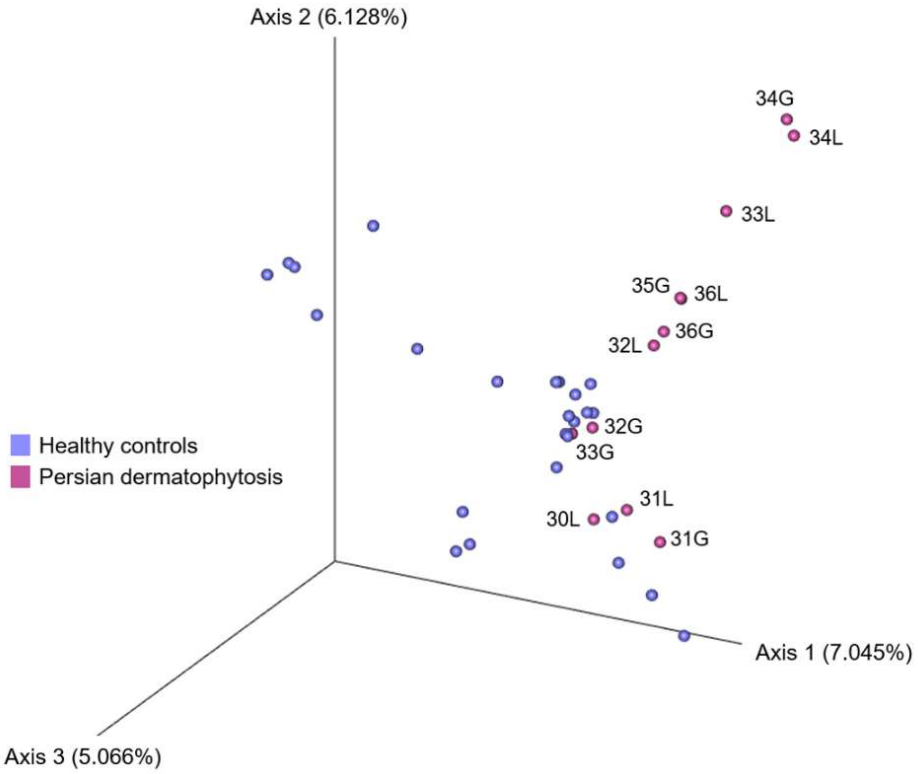

Figure 3. Principle coordinate analysis (PCoA) plot of Bray-Curtis distance matrix comparing fungal communities on Persian cats with severe dermatophytosis to healthy control cats.
Fungal community structure of healthy control (Persian cats and domestic longhair cats) cats is mildly but significantly different from that of Persian cats with dermatophytosis ($R=0.14$, $p=0.05$). Persian cats with dermatophytosis are labeled with case number so that general swabs (G) and lesion swabs (L) from the same cat can be visualized relative to each other. Reprinted with permission from Myers et al. (2021).

2.3.3. Microbial community composition

The composition of fungal communities in Persian cats with dermatophytosis and healthy cats were similar, with the exception of *Microsporum* sp., which was identified on the skin of all clinically affected cats but not on the controls (Figure 4). *Microsporum* sp. relative abundance in cases ranged from 3% to 88% with an average of 8% in general skin swabs and 29% in lesion swabs. In addition to a higher relative abundance of *Microsporum* sp. and its parent taxa, LEfSe analysis identified a higher relative abundance of *Bjerkandera* sp. in the general and lesion swabs from Persian cats with dermatophytosis. However, this taxa was only identified in three cats enrolled at the same clinic and may therefore be specific to that clinic or geographic location. While not significantly differentially abundant, *Candida* sp. and *Debaryomyces* sp. also appeared to have higher relative abundance in these three cats (Figure 4). Across all cats, the most common fungal phyla, Ascomycota and Basidiomycota, were present at 47% and 46% average relative abundances, respectively. The most abundant families across all cats were *Malasseziaceae*, *Didymosphaeriaceae*, and *Aspergillaceae*. The most common fungal genus on both affected and healthy cats was *Malassezia*, with an average relative abundance of 15%.

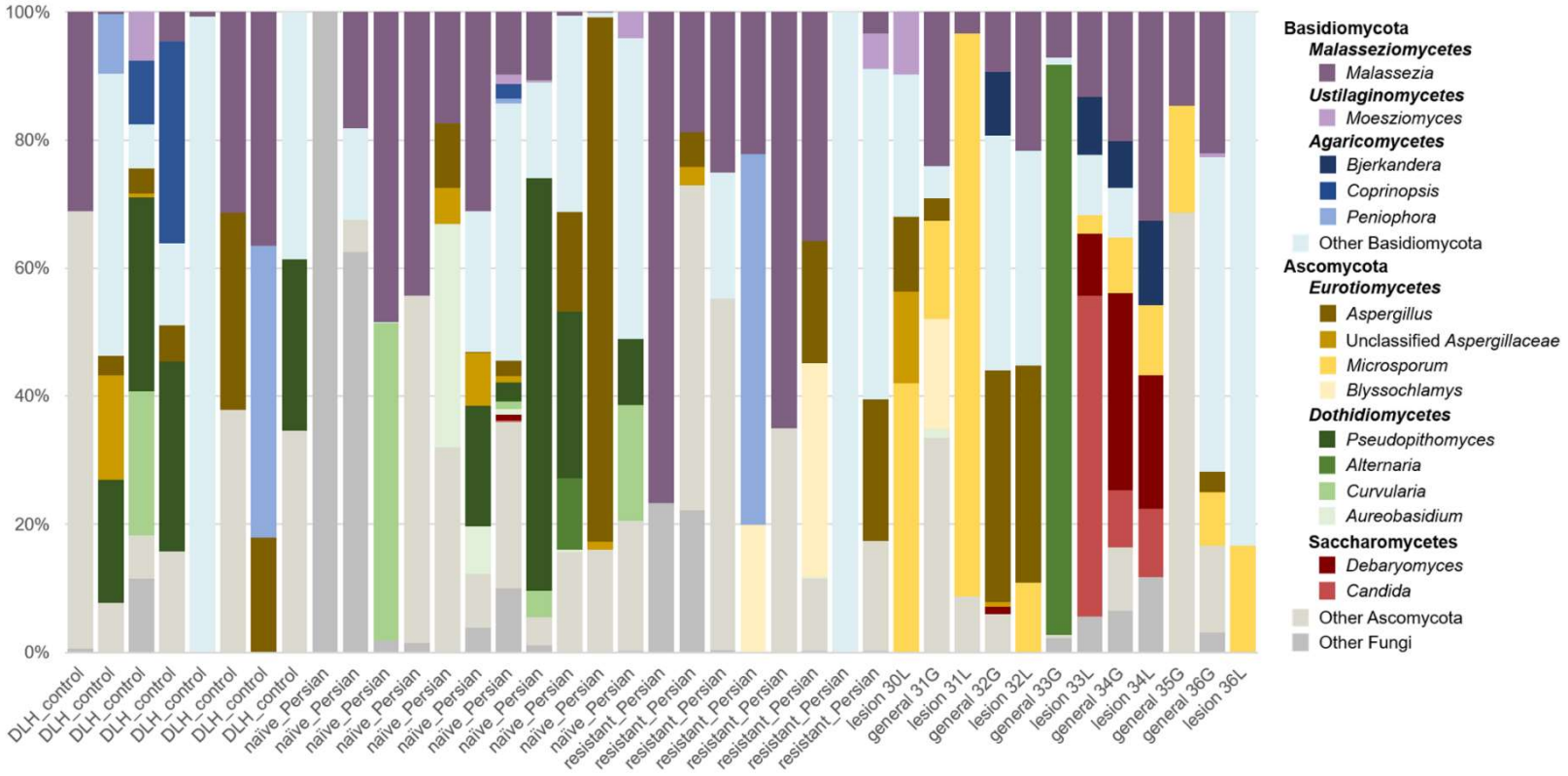

Figure 4. Relative abundance of fungal taxa on the skin of all cats.
Domestic longhair controls are referred to as 'DLH control', Group 1 Persian cats are referred to as 'naïve Persian', Group 2 Persian cats are referred to as 'resistant Persian', and each case of Group 3 severe dermatophytosis is identified by sample name so that lesion and general swabs from the same cat can be compared. Cases 32, 33, and 34 were enrolled at approximately the same time from the same clinic in Italy. Reprinted with permission from Myers et al. (2021).

The relative abundance of bacterial taxa in each sample are shown in Figure 5. LEfSe analysis identified several bacterial taxa that had significantly higher relative abundance in cases versus controls (Figure 6); however, this was based on only five swabs from cases (two general swabs and 3 lesion swabs). Further, the majority of taxa identified as differentially abundant are unique to the general and lesion swab from Case 34, and these taxa may be specific to that particular clinic or geographic region. When healthy Persian cats were compared with healthy DLH cats, LEfSe analysis identified *Corynebacteriaceae* as more abundant on Persian cat skin and *Moraxella* as more abundant on DLH skin (Figure 7). Average relative abundances of *Moraxella* species were <1% in both DLHs and Persian cats however.

Across all cats, the main bacterial phyla identified were Actinobacteria (mean relative abundance = 44.8%), Proteobacteria (28.2%), Firmicutes (12.1%), and Bacteroidetes (10.4%). The most abundant families across all cats were *Corynebacteriacea* (19.7%), and *Propionibacteriaceae* (13.9%). The most common genus on both affected and healthy cats was *Corynebacterium*. *Corynebacterium* was found at an average relative abundance of 24% on Persian cats specifically, but only 2.4% on DLH cats. However, two healthy Persian control cats from the same household both had a bacterial microbiota composed of >97% *Corynebacterium*, skewing the average relative abundance in Persians cats. If these two cats are excluded, the average relative abundance of *Corynebacterium* in Persian cats is still higher than DLH cats at 16.0%.

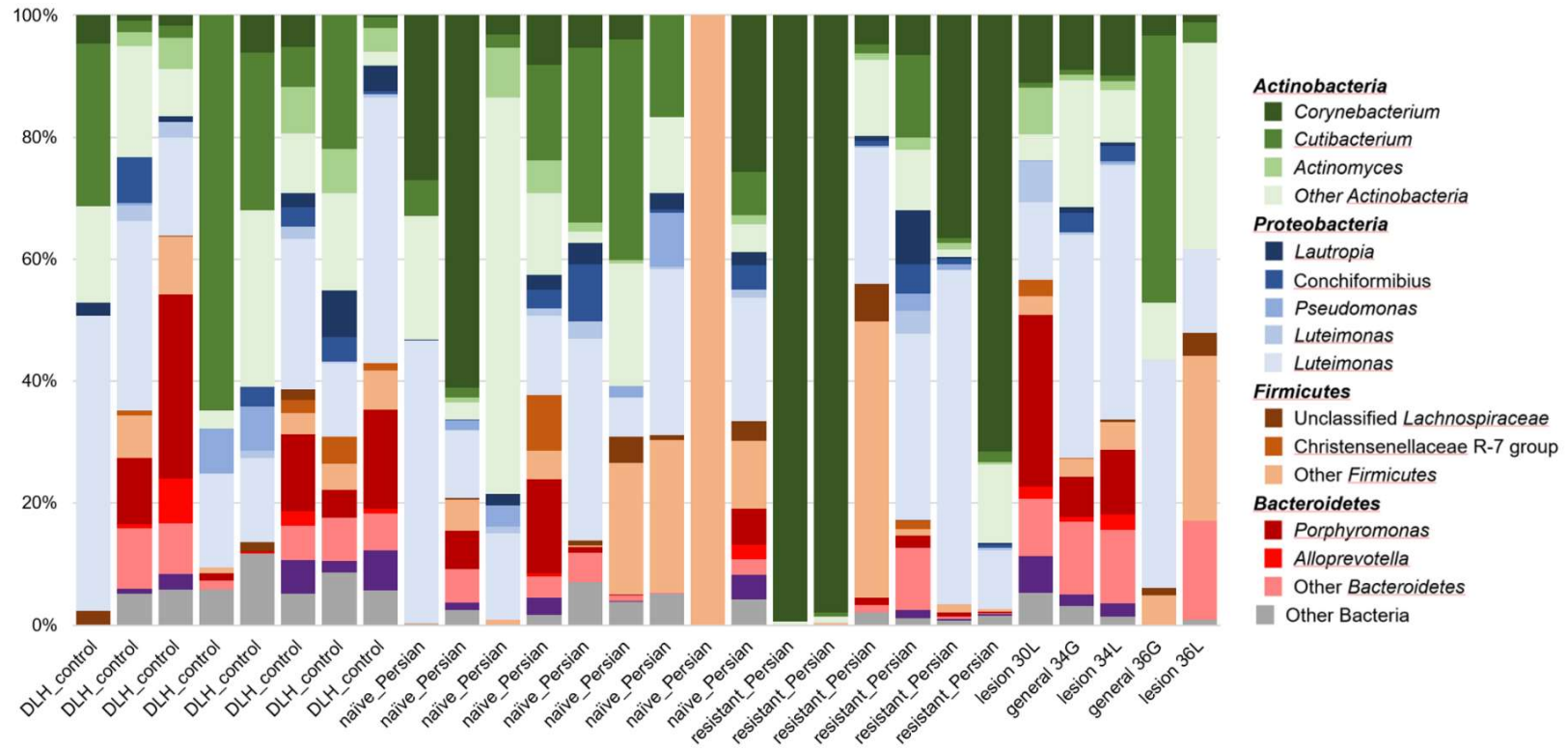

Figure 5. Relative abundance of bacterial taxa on the skin of all cats.
Domestic longhair controls are referred to as 'DLH control', Group 1 Persians are referred to as 'naïve Persian', Group 2 Persians are referred to as 'resistant Persian', and each case of Group 3 severe dermatophytosis is identified by sample name so that lesion and general swabs from the same cat can be compared. Reprinted with permission from Myers et al. (2021).

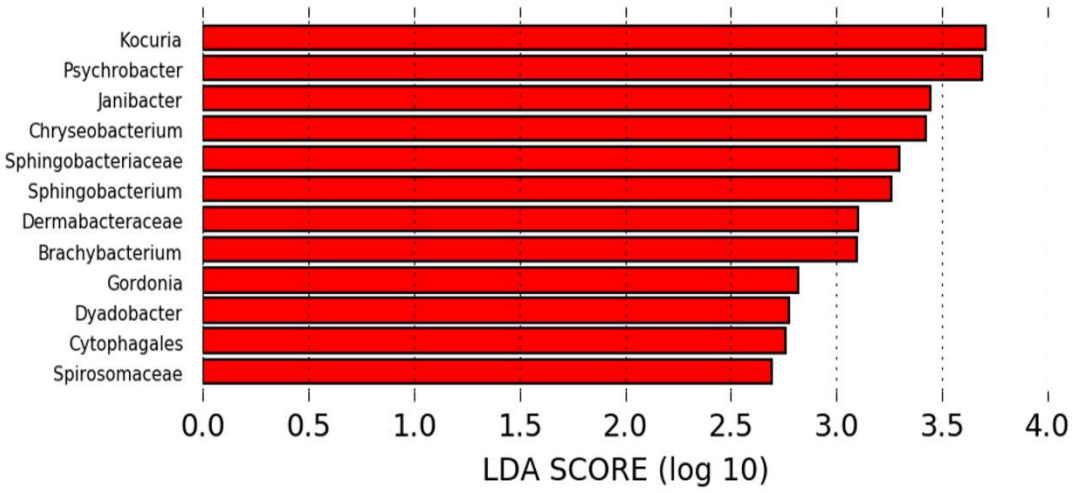

Figure 6. Bacterial taxa more differentially abundant on Persians with severe dermatophytosis than on all healthy control cats.
Plot created using LEfSe (LDA>2.5, p<0.01). Reprinted with permission from Myers et al. (2021).

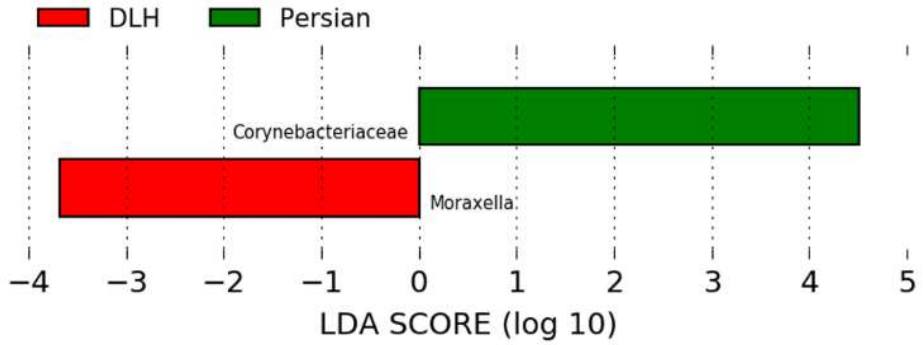

Figure 7. Bacterial taxa differentially abundant on healthy Persian cats compared with healthy control cats.
Plot created using LEfSe (LDA>2.5, p<0.01). Reprinted with permission from Myers et al. (2021).

2.3.4. Absolute abundance of fungal DNA

Quantitative PCR targeting the ITS1 region revealed that swabs from Persian cats with dermatophytosis exhibited higher estimated absolute abundance of fungal DNA than healthy cats, as evidenced by significantly lower Cq values (Figure 8). Significance was maintained over a range of sample dilutions (undiluted p=0.018; 8-fold dilution p=0.016; 64-fold dilution p=0.010).

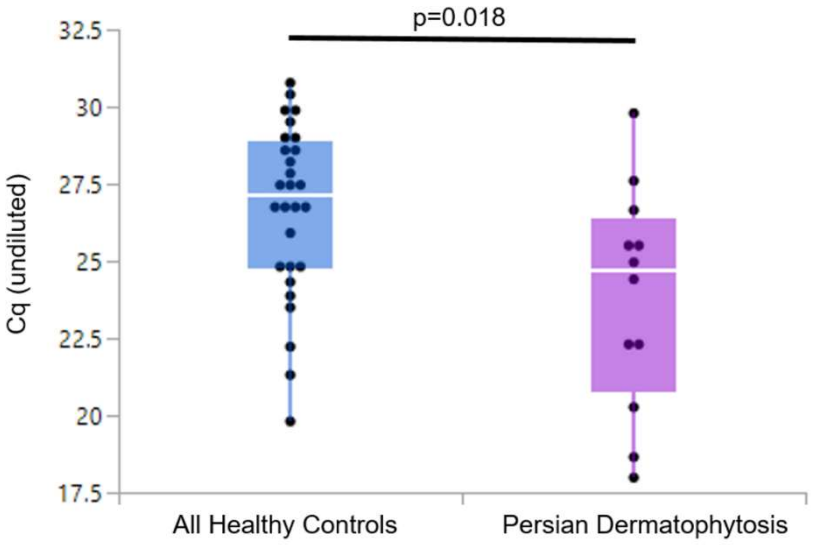

Figure 8. Absolute abundance of fungal DNA.
Plot of qPCR results from undiluted sample providing an estimate of absolute abundance of fungal DNA in samples from Persian cats with severe dermatophytosis (n=12) and healthy control cats (Persian cats and domestic longhair cats, n=28). Lower Cq values indicate higher estimated absolute abundance of fungal DNA. Persian cats with dermatophytosis exhibit significantly higher estimated absolute abundances of fungal DNA. Reprinted with permission from Myers et al. (2021).

2.3.5. Culture results and detection of asymptomatic carriers

Microsporum canis was cultured from all of the Group 3 Persian cases. *M. canis* was also cultured from two asymptomatic Persian cats that were housed in an environment known to be contaminated with dermatophytes. Less than five colonies were observed on the culture plates of these two cats, consistent with asymptomatic carriage of spores due to environmental contamination (Moriello et al. 2017). NGS failed to detect *M. canis* DNA from skin swabs of these two cats. No other control cats were positive for dermatophyte growth in culture. NGS did detect *Trichophyton rubrum* on one culture-negative, asymptomatic Persian control at a relative abundance of 9%. *T. rubrum* was found at 4% relative abundance in this cat's environment.

2.3.6. Direct colony PCR results

In two cases (case 32 and case 35), culture revealed colonies with morphologic features of *Microsporum canis* but without significant sporulation to confirm identification. Direct colony PCR and sequencing in both of these cases yielded sequences with 100% identity to *Microsporum canis* only.

2.3.7. Dermatophytes in the environment

Swabs of the home environment exhibited significantly higher fungal alpha diversity than samples obtained from feline skin (p-value <0.0001 for Shannon, observed ASVs, and Pielou's evenness). Of the two environmental samples obtained from Persian cats with dermatophytosis, both contained *Microsporum* DNA at relative abundances of

2% and 3%, respectively. Of the 11 environmental swabs obtained from Persian control cats, none had detectable *Microsporum* DNA, but two had *Trichophyton rubrum* DNA at 4% and <1% relative abundance.

2.4. Discussion

Previous research has not explained the increased incidence and severity of dermatophytosis in Persian cats. The influence of the cutaneous microbiota was examined here given that changes to the host microbiota are associated with several skin diseases in humans and animals. NGS successfully identified *Microsporum* sp. DNA from all cases of Persian cat dermatophytosis and from none of the healthy control cats. We did not identify an underlying fungal dysbiosis associated with dermatophytosis in this breed. Furthermore, no significant differences were identified in the bacterial microbiota between cases and controls, although only a few samples had enough bacterial sequences that could be used for downstream analysis. This suggests that alterations in the cutaneous microbiota, aside from *M. canis* itself, do not play a role in pathogenesis. The idea that the microbiome can be a host defense mechanism is well established (Stacy and Belkaid 2019); however, the microbiota of these cats does not appear to play a role in defense against dermatophytes. These results do indicate that NGS (ITS amplicon sequencing) is capable of consistently identifying dermatophytes on the hair and skin of clinically affected cats.

We expected to see decreased alpha diversity from lesions of dermatophytosis, as a previous culture-based study showed that saprophyte growth decreased to zero as

lesions progress over time (Moriello 1991). Additionally, two studies evaluating the microbiota of humans with tinea pedis (dermatophyte infection of the feet) showed decreased fungal diversity on lesional skin (Liu et al. 2019; Wang et al. 2018). However, our findings indicate that fungal diversity was similar on dermatophyte lesions and normal skin. Overall, healthy control samples had low fungal diversity and were often composed of a few predominant taxa, which may explain the lack of significant difference in diversity between cases and controls.

The fungal microbiota of healthy Persian cats is not significantly different from that of the DLH cats included in this study. This was investigated due to previously described breed-related differences in feline microbiota compositions (Older et al. 2019). There does not appear to be any unique features of the normal Persian cat fungal microbiota that might explain the increased incidence and severity of dermatophytosis. Importantly, the normal Persian cat microbiota does not contain *M. canis*.

M. canis was cultured from the hair coat of two Group 2 asymptomatic Persian cats that occupied the same environment as another Persian cat with severe dermatophytosis. Few colonies of *M. canis* grew on the culture plates from these cats, and these findings are consistent with asymptomatic carriage of dermatophyte spores on the hair coat due to environmental contamination (Moriello et al. 2017). NGS did not detect *Microsporum* DNA on these cats; this is most likely due to a combination of low spore abundance and the sample collection method. While the Mackenzie toothbrush method samples the hair coat of the entire cat, the microbiome swabbing method used in this study samples only a small surface area of the skin while avoiding the hair as much

as possible. This swabbing method commonly used for NGS is therefore not likely to consistently detect low numbers of spores on the hair coat of asymptomatic carrier cats.

Regarding the environmental microbiota of Persian cats, the findings are as expected, with *Microsporum* DNA detected only in the environment of clinically infected cats (Moriello et al. 2017). *Trichophyton rubrum* DNA was detected in the environment of two Persian cats and on the hair coat of one of those cats. This is an anthropophilic dermatophyte typically associated with human infections (including foot and nail fungal infections), and it has been shown previously that cats may carry this dermatophyte asymptomatically (Moriello et al. 2017). In these two Persian cat households, we suspect that *T. rubrum* was spread to the environment and subsequently the hair coat of a cat by an infected human.

A key limitation of this study is the limited number of cases, with three of the seven cases in Group 3 enrolled from one clinic in Italy. The microbiota of these cats contained unique taxa, but effects of geography or presence of environmental fungi in that particular clinic may explain these differences rather than an association with dermatophytosis. Inclusion of more cases from various locations would have been ideal. An additional limitation was the treatment of three cases with oral and topical antifungal drugs within one month of sample collection. This may have altered the diversity and structure of microbial communities, although dermatophytes were still detected on all three cats via NGS and culture. Given the low sample size and lack of high-quality bacterial microbiota data, further work may be needed to confirm whether the Persian skin microbiome plays a role in development of dermatophytosis.

In summary, the microbiota of Persian cats afflicted with dermatophytosis is different from healthy cats only in the increased abundance, absolute and relative, of *Microsporum* sp. No other significant differences were identified to indicate that an underlying dysbiosis exists. This study further supports that *M. canis* is not a component of the normal cat microbiota or of the normal Persian cat microbiota specifically. Other contributors to the increased incidence and severity of dermatophytosis in Persian cats should be sought, such as primary immunodeficiency, ineffective grooming, or unique features of Persian cat hair.

3. AN ANCIENT HAPLOTYPE CONTAINING ANTIMICROBIAL PEPTIDE GENE VARIANTS IS ASSOCIATED WITH SEVERE DERMATOPHYTOSIS IN PERSIAN CATS

3.1. Introduction

Superficial fungal infections of the hair, skin, and nails affect an estimated 1 billion people globally and are the most common type of fungal infection in the world. These infections are most often caused by fungi known as dermatophytes, and the infection itself may be referred to as dermatophytosis, tinea, or a more commonly known name—ringworm (Bongomin et a. 2017). While the disease is generally mild and self-limiting, its impact on human and animal welfare can be enormous (Narang et al. 2019). A large, ongoing epidemic of treatment-resistant dermatophytosis in India has called attention to the serious economic and welfare implications of this disease and stimulated more research on pathogenesis and treatment (Narang et al. 2019; Das et al. 2020; Patel et al. 2020).

Dermatophytes rely upon keratin as a source of nutrition. Ancestral dermatophytes gleaned this keratin primarily from soil, but recent adaptive radiation of this lineage has resulted in fungi that are adapted to keratins of specific host species (de Hoog et al. 2017; Wu et al. 2009; Zheng et al. 2020). Anthropophilic dermatophytes, such as those that cause athlete's foot and jock itch, are adapted to human keratins, while zoophilic dermatophytes are adapted to specific animal keratins (Merkhofer and Klein

2020). *Microsporum canis* prefers the dog and cat as its primary host species but is commonly transmitted to humans (Moriello et al. 2017).

Most dermatophyte infections are mild; however, severe and even fatal cases are occasionally reported (Rouzaud et al. 2015; Lanternier et al. 2013). In severe cases, the infection may become chronic, cover a large area of the body (extensive infection), and/or penetrate beyond the epidermis into the dermis and other tissues (deep infection). In humans, monogenic inborn errors of immunity have been shown to cause severe dermatophytosis, including autosomal recessive mutations in *CARD9* and autosomal dominant mutations in *STAT1* (Lanternier et al. 2013; van de Veerdonk et al. 2011; Glocker et al. 2009; Nielsen et al. 2015). Reports of genetic variation contributing to disease susceptibility rather than severity also exist, although full functional validation of these variants is lacking (Jaradat et al. 2015; Abdel-Rahman and Preuett 2012).

Persian cats are more likely than other breeds to develop dermatophytosis—including chronic, extensive, and/or deep infection—caused by the dermatophyte *M. canis* (Moriello et al. 2017; Lewis et al. 1991) (Figure 9). A genetic component to susceptibility and/or severity of disease has long been suspected in this breed, supported by observations that particular Persian catteries housing genetically related cats have significantly higher incidence of chronic disease than others (DeBoer and Moriello 1993). A recessive mode of inheritance is suspected given that severe, deep infections are relatively isolated to the Persian breed despite the Persian being used in the development of many other breeds of cat. Elucidating the genetic underpinnings of severe dermatophytosis in the Persian cat is likely to translate into better understanding

of the pathogenesis and treatment of dermatophytosis in other species, including humans. The objective of this study was to identify genetic variants associated with severe dermatophytosis in Persian cats using WGS. We further investigated the function and evolution of a key, skin-expressed AMP gene found within a divergent and disease-associated haplotype.

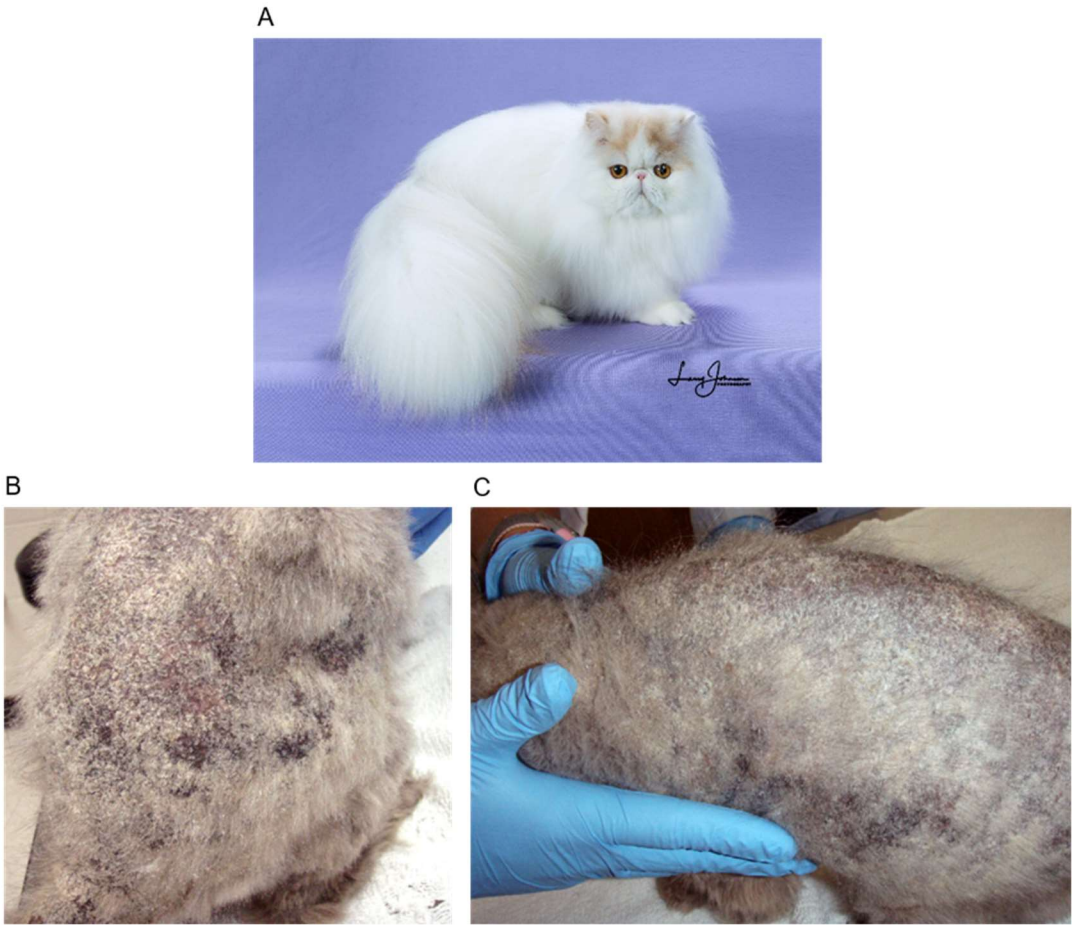

Figure 9. Macroscopic changes of a severe case of dermatophytosis in a Persian cat compared to a normal Persian cat.
(A) A healthy, modern Persian cat with full hair coat. Photo courtesy of Larry Johnson. (B-C) Diffuse hair loss and scaling on the dorsum of a Persian cat with severe (chronic and extensive) dermatophytosis.

3.2. Results

3.2.1. A locus associated with severe dermatophytosis contains immune gene variants

All Persian cat whole genome sequencing data was uploaded to the NCBI Short Read Archive under BioProject PRJNA704916. GWAS performed on variants called from the whole-genome sequencing data revealed a single peak of markers surpassing the Bonferroni correction threshold on chromosome F1, with the most significant markers having a p-value of 1.51x10-10 (Figure 10A). Upon closer inspection, this peak marked the location of a ~1 Mb haplotype block that was homozygous in 8/10 Persian cats with severe dermatophytosis (including the two cats with concurrent pseudomycetoma) and 0/16 Persian control cats (Figure 10B). This peak remained the only significant association when the GWAS was repeated using only the 8 control cats with confirmed exposure to dermatophytes without development of severe disease (Figure 11). The frequency of this allele was 90% among cases and 18.75% among all controls, as 6 controls were heterozygous for the allele. This haplotype block contains 42 genes, 8 of which contain disease-associated non-synonymous SNVs (Table 7). Half of these are well-characterized immune genes, including a cytokine receptor gene and AMP genes: *IL6R*, *S100A15*, *S100A12*, and *S100A9*.

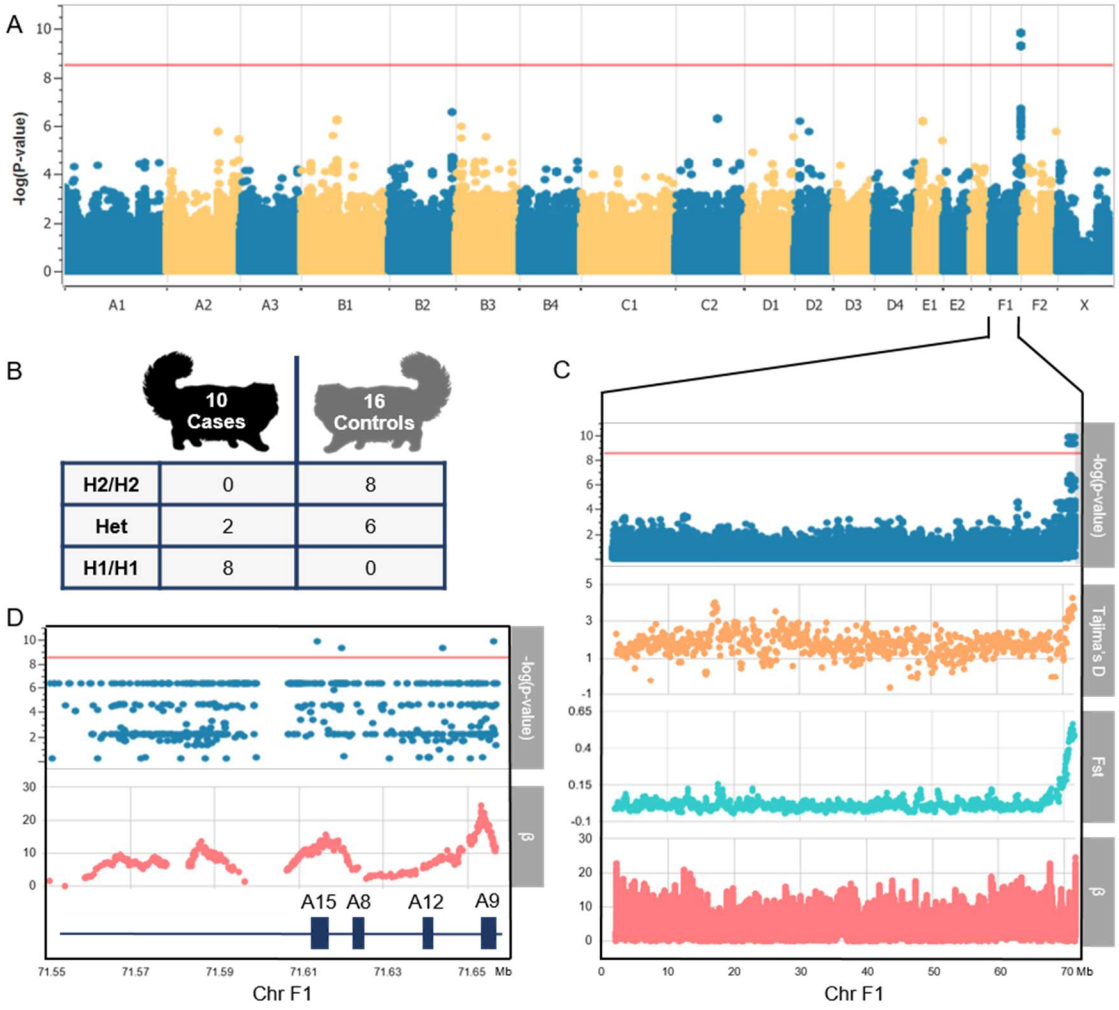

Figure 10. Genome-wide association analysis of Persians with and without severe dermatophytosis and evidence of divergent haplotypes under balancing selection. (A) Manhattan plot depicting single locus linear mixed model output for 10 Persian cat cases of severe dermatophytosis and 16 Persian cat controls. A locus on chromosome F1 achieves genome wide significance of p-value=1.51×10^{-10}. The Bonferroni-corrected significance threshold of p-value=3.30 x 10-9 is shown in red. (B) Table depicting the genotypes of cases and controls for the disease-associated locus on F1. H1 refers to haplotype 1 and H2 refers to haplotype 2. 'Het' is short for heterozygous and represents the genotype H1/H2 as well as genotypes H3/H4 and H1/H6 identified in two control cats.(C) A Manhattan plot depicting the entirety of chromosome F1 is shown along with Tajima's *D*, Weir and Cockerham's Fst, and the β statistic for detection of long-term balancing selection. (D) A regional Manhattan plot depicting the last ~100 kb of chromosome F1 is shown along with β and the gene annotation. Within the disease associated locus, β is most elevated over the S100A AMP genes, *S100A9* (A9) and *S100A15* (A15).

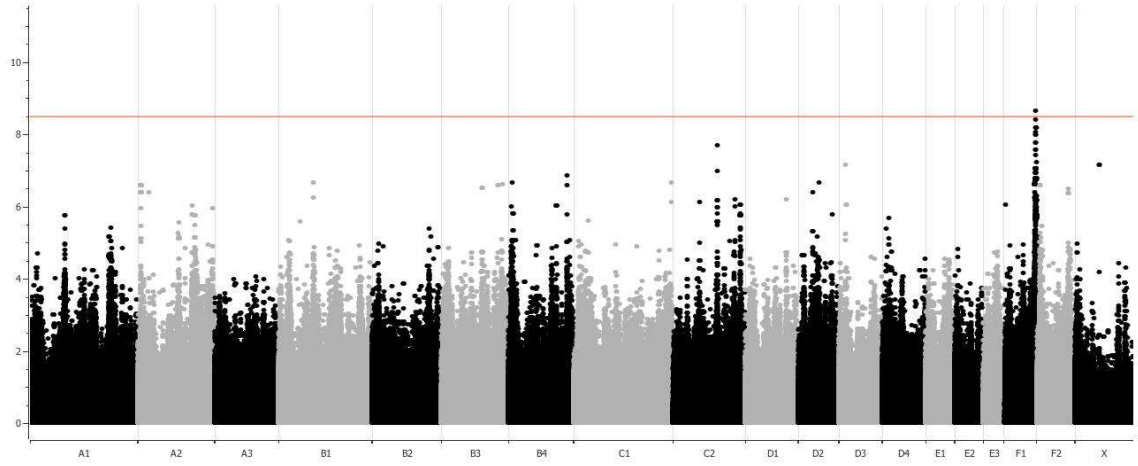

Figure 11. Genome-wide association analysis of Persians with and without severe dermatophytosis, including only those control cats with prior confirmed exposure to dermatophytes.

Manhattan plot depicting single locus linear mixed model output for 10 Persian cat cases of severe dermatophytosis and 8 Persian cat controls that were previously exposed to dermatophytes without developing severe disease. As in the GWAS performed with all 16 control cats, a single peak of SNPs on chromosome F1 surpasses the Bonferroni-corrected significance threshold of p-value=3.30 x 10^{-9}.

Table 7. Non-synonymous substitutions between case and control cats within the disease-associated locus.

Gene	Genomic coordinates	NCBI protein ID	Amino acid alteration	PROVEAN score	Effect prediction
IL6R	F1:70945999	XP_023103841.1	T287A	-0.357	neutral
NUP210L	F1:71150962	XP_019678071.2	V590I	0.018	neutral
NUP210L	F1:71168597	XP_019678071.2	S968P	-3.015	deleterious
NUP210L	F1:71179382	XP_019678071.2	A1358T	-0.406	neutral
NUP210L	F1:71179388	XP_019678071.2	R1360G	2.137	neutral
CREB3L4	F1:71210681	XP_003999812.1	C269R	1.989	neutral
CRTC2	F1:71227249	XP_003999815.3	S236A	-0.908	neutral
CRTC2	F1:71229627	XP_003999815.3	Q517P	-1.526	neutral
S100A4	F1:71536030	XP_003999828.1	Y17H	4.92	neutral
S100A15	F1:71612744	XP_019676968.1	A43V	1.242	neutral
S100A12	F1:71639972	XP_006943210.2	W17R	3.935	neutral
S100A12	F1:71640026	XP_006943210.2	E35Q	1.444	neutral
S100A12	F1:71640518	XP_006943210.2	E67G	0.245	neutral
S100A12	F1:71640554	XP_006943210.2	C79S	0.285	neutral
S100A9	F1:71653999	XP_003999832.3	A109T (A87T)	2.004	neutral
S100A9	F1:71654029	XP_003999832.3	K99E (K77E)	1.999	neutral
S100A9	F1:71654035	XP_003999832.3	D97N (D75N)	-0.054	neutral
S100A9	F1:71654085	XP_003999832.3	V80A (V58A)	1.045	neutral
S100A9	F1:71654088	XP_003999832.3	T79N (T57N)	-0.029	neutral
S100A9	F1:71654104	XP_003999832.3	E74Q (E52Q)	-0.095	neutral
S100A9	F1:71655946	XP_003999832.3	E64K (E42K)	-0.916	neutral
S100A9	F1:71655961	XP_003999832.3	M59L (M37L)	0.489	neutral
S100A9	F1:71655969	XP_003999832.3	P56Q (P34Q)	3.236	neutral
S100A9	F1:71655985	XP_003999832.3	A51P (A29P)	3.156	neutral
S100A9	F1:71655990	XP_003999832.3	G49E (G27E)	-6.244	deleterious
S100A9	F1:71656006	XP_003999832.3	H44Y (H22Y)	3.497	neutral
S100A9	F1:71656065	XP_003999832.3	A24E (A2E)	-0.978	neutral

NOTE.—Amino acid alterations are reported as the residue found in the FCA_H2 (control) haplotype followed by the residue in the FCA_H1 (case) haplotype. For *S100A9*, the text in parenthesis corrects for a putatively mis-annotated start site in the feline reference genome.

3.2.2. Divergent S100A9 haplotypes and comparison with wild felid haplotypes

S100A9 exhibited the highest level of divergence between cases and controls and was considered a compelling candidate gene given its previously described role in antifungal immunity and its reported epidermal expression in other species (Clark et al. 2016; Urban et al. 2009; Chessa et al. 2020). For these reasons, we focused on *S100A9* for further analysis. Six distinct *S100A9* haplotypes were identified in the general domestic cat population, including the haplotype that was homozygous in 8/10 Persian cat cases (Domestic cat H1, hereafter referred to as the case haplotype) and the most frequent haplotype identified in Persian cat controls (Domestic cat H2, hereafter referred to as the control haplotype) (Figure 12A-C). Both the case and control haplotypes were also identified in a wild-caught Asiatic wildcat (*Felis silvestris ornata*) from Tajikistan. The case and control *S100A9* haplotypes are highly divergent for two populations of the same species, sharing 97.91% nucleotide sequence identity across 2,864 base pairs and 89.26% identity across 135 amino acids. This protein, though relatively small, exhibited 13 amino acid substitutions between cases and control haplotypes (Figure 13A, Figure 14).

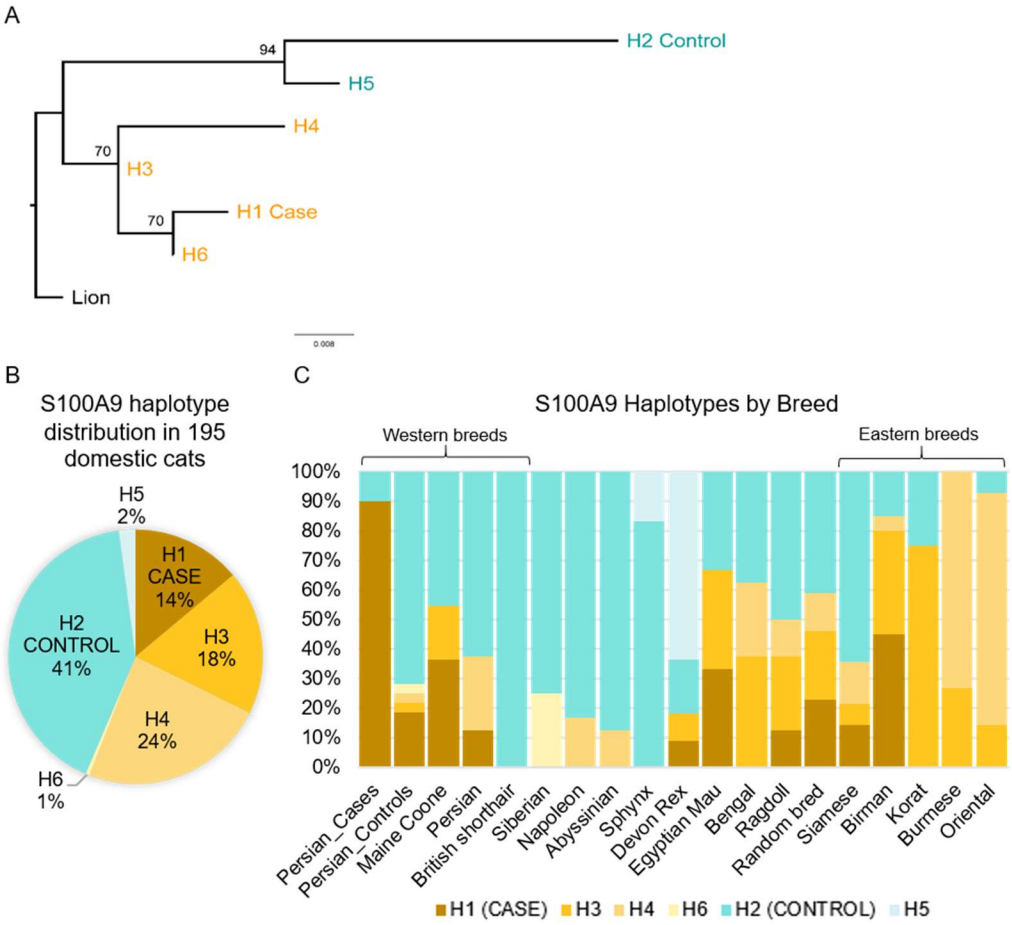

Figure 12. S100A9 haplotype frequencies in the general cat population.
(A) Maximum-likelihood phylogenetic tree inferred from the amino acid sequence of 6 distinct domestic cat S100A9 haplotypes with the lion as the outgroup. Bootstrap support values are given on nodes. (B) Overall distribution of S100A9 haplotypes in 195 domestic cats of varied breed and background. Haplotypes that cluster together with the Persian case haplotype (H1) are shaded in warm colors while haplotypes that cluster with the Persian control haplotype (H2) are shaded in cool colors. (C) Relative frequency of haplotypes in various cat breeds. Labels for Persian_Controls and Persian_Cases represent the haplotype frequencies for the Persian cats enrolled in this study while the label for Persian represents Persian cats in the general cat population. Haplotypes H3 and H4 predominate in cat breeds previously determined to be of Eastern origin. Breeds were included only if represented by at least two individuals (4 haplotypes).

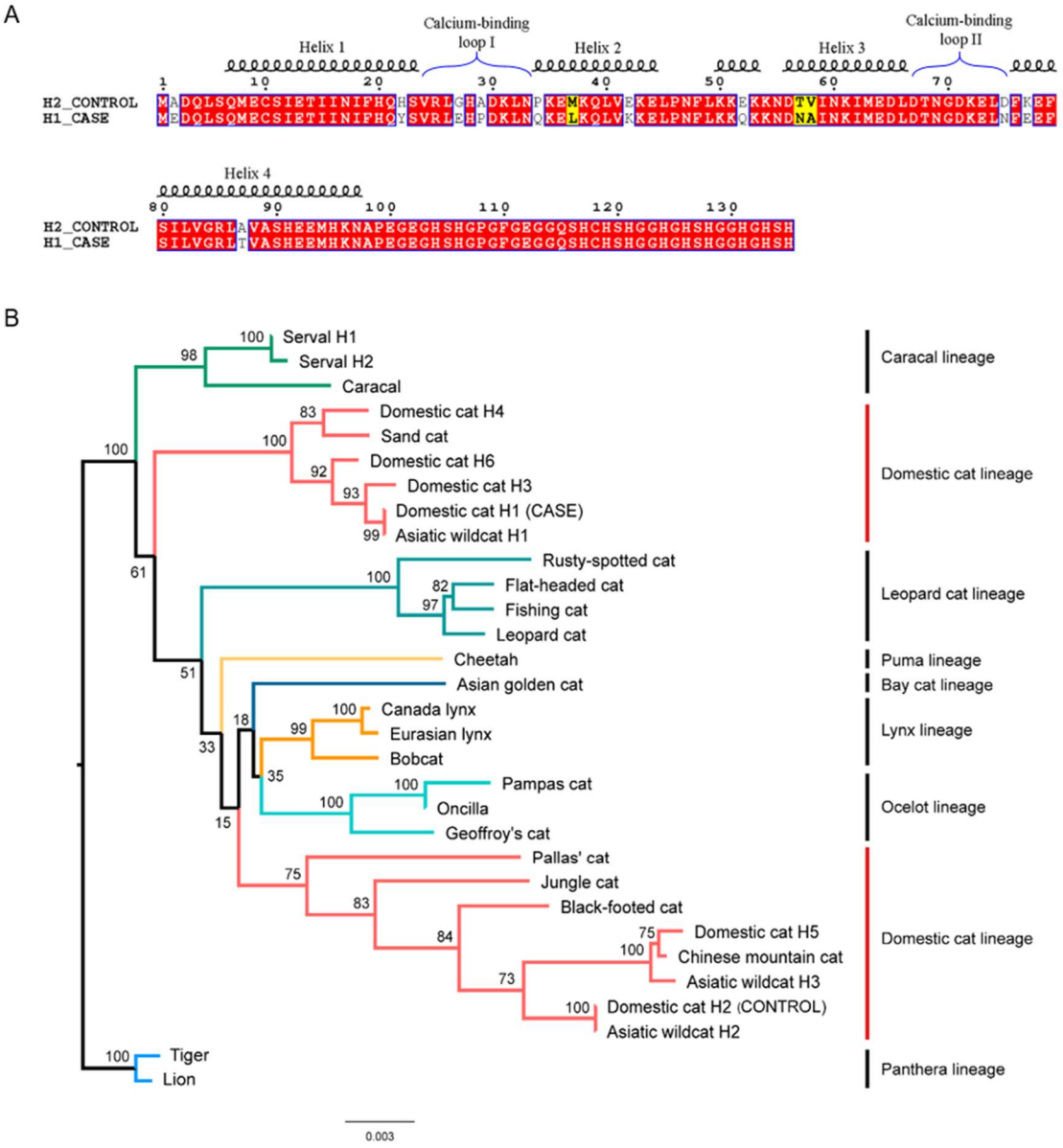

Figure 13. Highly divergent S100A9 haplotypes and comparison with wild felids. (A) Amino acid sequence alignment and secondary structure depiction of the divergent Persian cat case and control S100A9 haplotypes, created with ESPript 3.0. Conserved residues are boxed in red while similar residues are in bold text and boxed in yellow. (B) Maximum-likelihood phylogenetic tree inferred from the phased *S100A9* nucleotide sequences of 22 wild felids and the domestic cat haplotypes. Bootstrap support values are given on nodes. The domestic cat lineage is split across the tree: the Persian cat case haplotype (Domestic cat H1) clusters with the sand cat near the root of the tree while the control haplotype (Domestic cat H2) is found in the expected location for the domestic cat lineage.

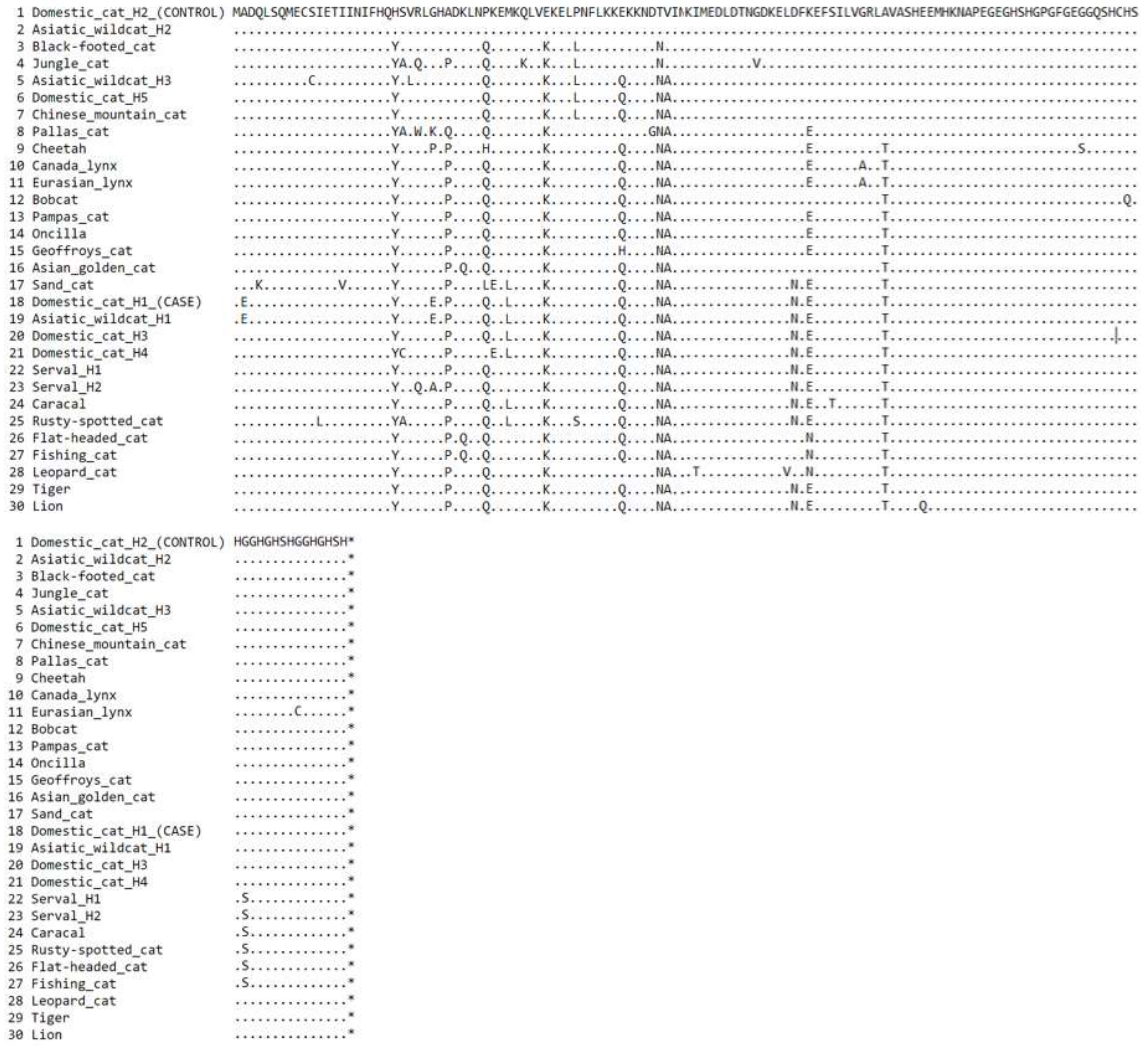

Figure 14. S100A9 amino acid alignment for wild felids and domestic cat haplotypes.

To explore the origin of the divergent alleles, a maximum-likelihood phylogenetic tree was inferred from the phased *S100A9* nucleotide sequences of 22 wild felids and the six domestic cat *S100A9* haplotypes (Figure 13B). The control haplotype was found in its expected phylogenetic position with haplotypes from other species of the domestic cat lineage (Li et al. 2016, 2019). However, the Persian case haplotype and the *Felis margarita* (sand cat) haplotypes formed a unique and highly divergent cluster from other *Felis* haplotypes as well as all other Felidae lineages. An approximately unbiased (AU) test confirmed that this placement deviates significantly from the Felidae species tree topology (p-value=6.19x10-7). While the Persian case *S100A9* nucleotide sequence was only 97.91% identical to the control haplotype, it shared 99.27% identity with the sand cat sequence. The amino acid sequence of the case haplotype shared 89.26% identity with the control haplotype but 95.04% identity with the sand cat sequence. Overall, the Persian case haplotype is more diverged from the Persian control haplotype than from the sand cat haplotype (Li et al. 2016). Elsewhere in the phylogeny, there is little deviation from the species tree as would be expected with incomplete lineage sorting; therefore, ancient hybridization and introgression of this allele into ancestors of the sand cat and domestic cat populations is a more plausible explanation.

There is no evidence that genome assembly errors or copy number variation interfered with read mapping at this locus to explain the increased non-synonymous variation. Alignment of raw reads from a case and control cat to a new, single-haplotype *Felis catus* genome assembly revealed no differences in alignment or haplotypes from the standard felCat9 assembly (Figure 15). CNVnator analysis of chromosome F1 did

not reveal gene duplications within the disease-associated locus. Many cats are homozygous for the case or control haplotype, providing further proof that paralogous genes are not leading to mis-mapping of reads at this locus—this phenomena should result in heterozygous sites.

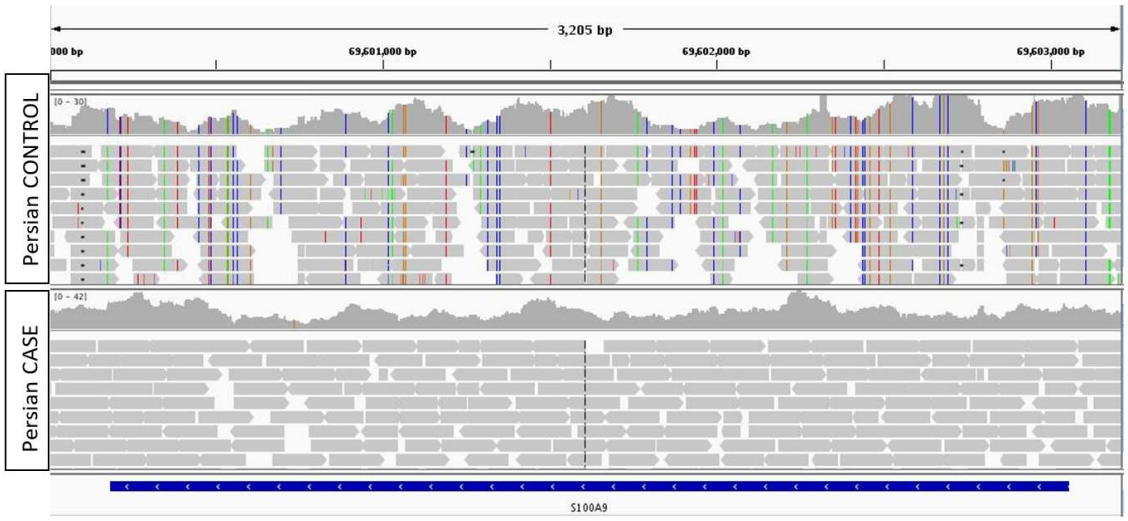

Figure 15. IGV output of raw sequencing reads from a Persian case and a Persian control cat aligned to a single-haplotype *Felis catus* genome assembly (BioProject ID PRJNA670214).
This single-haplotype genome has the Persian case haplotype (H1) at *S100A9*, hence the lack of SNVs in the Persian case alignment. The Persian control cat is homozygous for the control haplotype (H2). Marked variation between the case and control haplotypes is apparent.

3.2.3. S100A8/S100A9 skin expression during feline dermatophytosis

S100A9 and S100A8 dimerize in vivo to form the AMP known as calprotectin. Keratinocytes of 0/5 non-lesional domestic shorthair cats exhibited epidermal immunolabeling for S100A8/S100A9 (calprotectin) while keratinocytes of 10/10 cats (5 domestic shorthair cats and 5 Persian cats) with dermatophytosis exhibited moderate to strong, multifocal to diffuse epidermal immunolabeling (Figure 16, Figure 17). These findings demonstrate a clear association between dermatophyte infection and increased expression of calprotectin in feline keratinocytes. This provides indirect evidence that calprotectin plays a role in defense against dermatophytes at the skin surface. We were unable to obtain sufficient concentrations of DNA from these FFPE skin samples to perform *S100A9* genotyping.

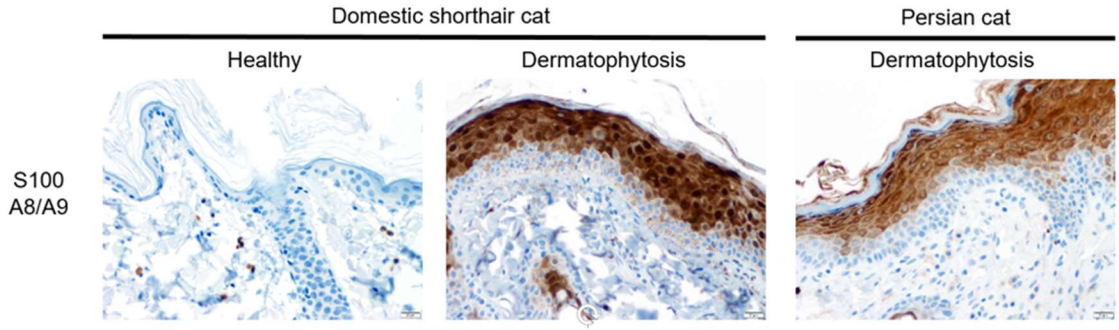

Figure 16. S100A8/S100A9 (calprotectin) immunohistochemistry performed on feline skin with and without dermatophytosis.
No immunolabeling of the epidermis was observed in healthy domestic shorthair cats. Both domestic shorthair cats and Persian cats with dermatophytosis exhibited strong immunolabeling of the epidermis, excluding the basal cell layer. S100A8/S100A9 immunohistochemistry.

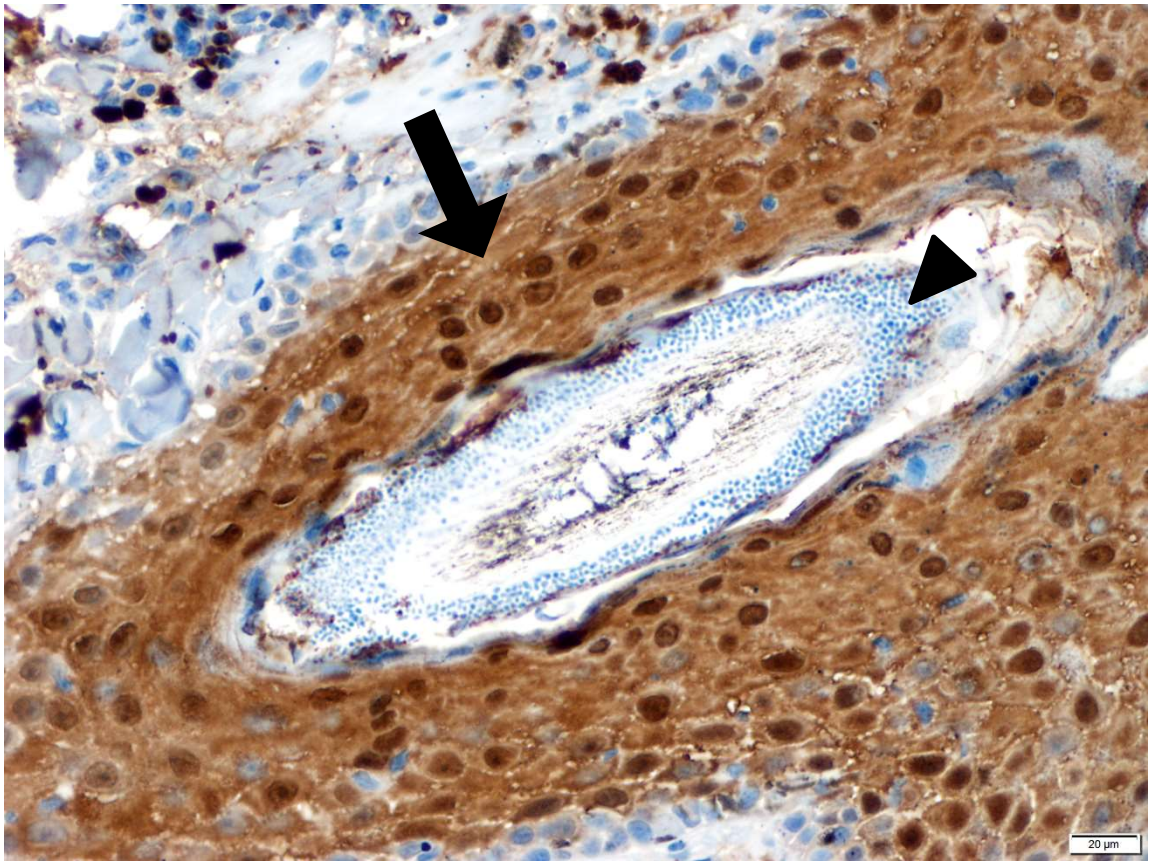

Figure 17. S100A8/S100A9 (calprotectin) immunohistochemistry performed on feline skin with dermatophytosis.
Hair follicle epithelium exhibits strong immunolabeling (black arrow). The hair within the follicle is engulfed in a layer of small, basophilic dermatophyte arthrospores (black arrowhead). Immunohistochemistry for S100A8/S100A9.

3.3. Discussion

Using whole-genome sequencing, we identified a highly divergent haplotype containing AMP genes that was significantly associated with severe dermatophytosis in Persian cats. In particular, the *S100A9* gene encoding a subunit of the AMP known as calprotectin was riddled with amino acid substitutions between case and control haplotypes. We demonstrate that calprotectin (S100A8/A9) is likely to be an important player in anti-dermatophyte defense at the skin surface where this protein is highly expressed during infection.

AMPs are an important component of the immune defenses of multicellular eukaryotes (Lazzaro et al. 2020). They are a highly diverse group of small proteins with activity against bacteria, fungi, and viruses (Lazzaro et al. 2020). Interestingly, AMPs were previously thought to have broad-spectrum activity against various pathogens; however, recent studies suggest a higher degree of specificity for particular pathogens and show that single amino acid substitutions can alter specificities (Lazzaro et al. 2020). The AMP calprotectin has been shown to exhibit activity against bacteria and fungi such as *Candida* sp. and *Aspergillus* sp., but studies evaluating its efficacy against dermatophytes are lacking (Clark et al. 2016; Sohnle et al. 1991; Steinbakk et al. 1990; Corbin et al. 2008). Calprotectin exerts antimicrobial effects by chelating transition metals such as Zn and Mn needed for microbial growth—this is termed nutritional immunity (Zygiel and Nolan 2018). Recently, however, Besold et al. (2018) demonstrated that calprotectin also inhibits bacterial growth through direct physical

interaction that does not involve metal withholding. The full mechanism for calprotectin's antimicrobial action is still being elucidated.

Although the Persian cat case allele of calprotectin appears to render these cats susceptible to severe *Microsporum canis* infections, we consider it likely that this allele would be beneficial against other pathogens, given its relatively high frequency in the domestic cat population. AMPs of many species have been described to evolve under pathogen-driven balancing selection that occurs as a result of an evolutionary arms race between pathogens and the immune genes they directly interact with (Chapman et al. 2016, 2019; Halldórsdóttir and Árnason 2015; Cagliani et al. 2008). Maintenance of divergent alleles within a population can serve as a defense mechanism for a population by providing a heterozygote advantage and/or provide a reservoir of alleles that may be useful in specific conditions/environments or against particular pathogens (Chapman et al. 2019). Interestingly, high levels of non-synonymous variation have been previously identified within S100A AMP genes of taurine cattle and yak, suggesting a similar scenario of divergent haplotypes as observed in cats (Luo et al. 2018).

We identified the divergent *S100A9* case and control alleles not only in domestic cats but also in an Asiatic wildcat (*Felis silvestris ornata*) from Tajikistan. Further, the case allele is similar to the sand cat (*Felis margarita*) allele, and together these alleles cluster much closer to the root of Felidae than expected. These findings indicate either introgression of the case allele into *Felis* species after an ancient hybridization event, long-term balancing selection, or a combination of the two (selection acting upon introgressed variation). We speculate that the haplotypes clustering in the clade with the

sand cat and Persian case haplotypes may have been adaptive in the arid desert environments inhabited by the sand cat and many of the *Felis silvestris* subspecies thought to be the predecessors of modern domestic cats (Yamaguchi et al. 2004). Arid regions are home to a different assortment of pathogens, and studies have shown that dermatophytes are more prevalent in warm, humid environments rather than arid conditions (Hamm et al. 2020; Wisal and Salim 2010; Gnat et al. 2020). In modern long-haired Persian cats that are not confined to the desert, however, the divergent *S100A9* allele may be maladaptive. Further tests to assess effectiveness of the divergent calprotectin protein against other common feline pathogens should be undertaken to clarify any potential benefit of this allele. Additional work should be done to characterize the frequency and severity of dermatophytosis in other cat breeds that carry the case haplotype.

The phenotype assessed in this study was that of chronic and extensive dermatophytosis in Persian cats despite appropriate veterinary-directed treatment. Due to small sample size, we were unable to specifically assess the phenotype of dermatophytic pseudomycetoma—a particular form of deep dermatophytosis that is also reported in humans (Berg et al. 2007; Castro-Echeverry et al. 2017). Only two Persian cat cases included in this study had concurrent pseudomycetoma. These cats were homozygous for the case haplotype, but a larger sample size is needed. The clinical and histologic appearance of pseudomycetoma is quite different from that of superficial dermatophytosis, and the immune genes and pathways involved may be different as well. Additional genotyping for pseudomycetoma cases is needed to determine if the

S100A9 case haplotype or closely-related haplotypes are associated with this specific phenotype.

Numerous AMPs are currently in clinical trials for treatment of disease in humans (Lazzaro et al. 2020; Mookherjee et al. 2020; Browne et al. 2020). There is burgeoning interest in engineering these peptides to increase specificity against particular pathogens, and they are expected to have less trouble with development of antimicrobial resistance (Souza et al. 2020). It would be interesting to investigate whether certain forms of calprotectin could be applied as a topical treatment for dermatophytosis.

In summary, a divergent haplotype on chromosome F1 containing S100A AMP genes is associated with development of severe dermatophytosis in Persian cats. If this haplotype is not found to confer any significant benefit against other pathogens, a genetic test could be easily created to identify cats with the case haplotype and to help adjust breeding programs. These findings open the door for future investigation into AMPs as treatment options for dermatophytosis in humans and animals. Alternate treatments are becoming more important as incidence of dermatophytosis continues to rise (Gnat et al. 2020).

3.4. Materials and Methods

3.4.1. Sample collection and whole-genome sequencing

An animal use protocol (IACUC 2018-0256 CA) was approved by the Texas A&M University Institutional Animal Care and Use Committee to enroll clinical cases

for this study. Study participants consisted of 26 adult Persian cats divided into 10 cases of severe dermatophytosis and 16 controls. Severe dermatophytosis was diagnosed by a veterinarian in all cases and was defined as chronic/recurrent infection covering a significant area of the body. In addition, two cases also had biopsy-confirmed dermatophytic pseudomycetoma, an uncommon form of deep dermatophytosis seen almost exclusively in Persian cats. Eight out of 10 cases had recurrence or continuation of infection despite receiving appropriate veterinarian-directed treatment; the remaining two cats could not be confirmed to have received appropriate treatment. Regarding the control cats, 8/16 cats had documented past exposure to dermatophytes (>6 months prior to sample collection) but no history of severe or chronic infection. The remaining control cats had no history of dermatophytosis, but exposure status was unknown.

Two buccal swabs (CytoSoft Cytology Brush, Medical Packaging Corporation, Camarillo, CA) were collected from each cat. DNA was extracted from buccal swabs within 1 week of sample collection using the salting out method and Gentra Puregene reagents (Qiagen, Hilden, Germany). Standard barcoded Illumina libraries were prepared for each cat using the NEBNext Ultra II FS DNA Library Prep Kit for Illumina and NEBNext Multiplex Oligos for Illumina (New England Biolabs, Ipswich, MA). Libraries were sequenced to an average of 14X depth on the Illumina NovaSeq platform (Illumina, Inc., San Diego, CA).

3.4.2. Variant calling and genome-wide association study

Data processing involved the following steps: 1) Quality and adapter trimming of raw reads with Cutadapt v1.18 (Martin 2011), 2) alignment of reads to the feline reference genome (felCat9) using BWA-mem v0.7.17 (Li 2013), and 3) variant calling with GATK v4.1.0.0 following the Broad Institute's best practices guidelines with the exception that hard filtering was performed rather than variant quality score recalibration (Poplin et al. 2018). Only biallelic SNPs were retained. SNPs with any missing genotypes or MAF ≤5% were removed, producing a final set of approximately 15.1 million SNPs.

To correct for cryptic population structure and relatedness, a linear mixed model approach, EMMAX (Kang et al. 2010), was used for the GWAS in the Golden Helix software package (Golden Helix, Bozeman, MT). We used a Bonferroni-corrected genome-wide significance threshold of 3.30×10^{-9} based on the number of variants called in our data set. Population stratification was characterized with a QQ plot. The PROVEAN v1.1.3 web-based tool was used to classify the effect of variants on protein function (score <-2.5 indicates deleterious effect) (Choi and Chan 2015). Outside of the disease-associated locus, genes known to be involved in fungal immune pathways or skin barrier function were examined manually in IGV (Robinson et al. 2017) for large deletions or other forms of copy number variation.

3.4.3. Population genetics and evolutionary comparisons

First, steps were taken to eliminate copy number variation and genome assembly errors as a cause of increased non-synonymous variation at the disease-associated locus. Raw Illumina reads for a case and control cat were aligned to a new, single-haplotype *Felis catus* genome assembly (BioProject ID PRJNA670214) (Bredemeyer et al. 2020) in order to rule out felCat9 assembly errors (such as collapse of repetitive or highly divergent sequence) in the region of the disease-associated haplotype. Additionally, CNVnator (Abyzov et al. 2011) was run for chromosome F1 to determine if sequence duplication could be contributing to increased sequence variation.

The sequence of *S100A9* was investigated among the general cat population using publicly available variant data for 195 domestic cats of various breeds and backgrounds. *S100A9* haplotypes were identified from this data via manual investigation of variant maps using Golden Helix (Golden Helix, Bozeman, MT). Haplotype frequencies were calculated overall and by breed.

Domestic cat *S100A9* haplotypes were compared with *S100A9* sequences of 22 wild felids. Illumina sequence data from each of the 22 wild felids was trimmed and aligned to the domestic cat reference genome (felCat9) using BWA-mem. The resulting BAM files were examined in IGV. For each felid, a fasta file of the full *S100A9* nucleotide sequence was extracted using ANGSD v0.925 (Korneliussen et al. 2014), and manual phasing was applied for those felids that had single nucleotide polymorphisms within this gene identified in IGV. Minimal phasing was needed as the majority of felids were homozygous or nearly homozygous for variants in this region. The phased wild

felid and domestic cat haplotypes were aligned and a maximum likelihood tree was constructed using IQ-TREE v1.6.12 (-m GTR+I+G -b 500) (Minh et al. 2020). An approximately unbiased (AU) test was also performed using IQ-TREE to determine if the *S100A9* gene tree was significantly different from the Felidae species-tree topology as inferred from low-recombining regions of the X-chromosome by Li et al. (2019).

To examine forces of natural selection acting upon *S100A9*, we evaluated Weir and Cockerham's Fst and Tajima's *D* for the Persian cats included in this study using VCFtools v0.1.16. We evaluated Tajima's *D* in 100 kb windows and Fst in 100 kb sliding windows across chromosome F1. We additionally calculated the beta statistic (β), designed to detect ancient balancing selection using BetaScan (default settings with the addition of -w 6000 and -fold options) (Siewart and Voight 2017). Repetitive regions and regions exhibiting copy number duplication, as identified by WindowMasker and CNVnator respectively, were masked for this analysis (Morgulis et al. 2006; Abyzov et al. 2011).

3.4.4. Immunohistochemistry

In order to assess and localize S100A8/S100A9 (calprotectin) expression in normal and affected feline skin, immunohistochemistry (IHC) was performed on archived FFPE cat skin using an antibody to human calprotectin that has been used extensively in various species including cats (Marsilio et al. 2014; Kipar et al. 2006). IHC was performed on skin from 5 healthy domestic shorthair cats, 5 domestic shorthair cats with dermatophytosis, and 5 Persian cats with dermatophytosis. Attempts were

made to extract DNA from these FFPE skin samples for PCR-based genotyping of the *S100A9* region; however, these samples did not yield enough quality DNA for accurate genotyping.

FFPE sections of feline skin were cut at 4 μm and mounted on charged slides. The sections were deparaffinized in xylene and rehydrated through graded alcohols. Antigen retrieval was performed by immersing the slides in a citrate buffer and heating them in a pressure cooker (Decloaking Chamber, Biocare Medical, Pacheco, CA). After retrieval, the slides were washed with tris buffer prior to beginning the immunostaining procedure. The immunohistochemical procedure was run on an automated platform (intelliPATH FLX, Biocare Medical). All incubations were run at room temperature. Endogenous peroxide activity was blocked by incubating the slides with hydrogen peroxide for 10 minutes. The sections were then incubated with the primary antibody (mouse anti-human Myeloid/Histiocyte Antigen, clone MAC 387, dilution 1:200, Agilent Technologies, Santa Clara, CA) for 30 minutes. Next, the slides were incubated with a polymer detection reagent (Mouse-on-Canine HRP Polymer, Biocare Medical) for 40 minutes. Sites of antibody-antigen interaction were visualized with a DAB chromogen (ImmPACT DAB Substrate kit, peroxidase, Vector Laboratories, Burlingame, CA). The sections were then counterstained with Mayer's hematoxylin. A negative control reagent (Universal Negative Control Serum, Biocare Medical) was substituted for the primary antibody for the negative control tissues. Each sample was assessed for intensity and distribution of keratinocyte staining.

4. CONCLUSIONS

This dissertation research attempted to identify reasons for the increased severity of dermatophytosis in Persian cats using a combination of genomic and metagenomic approaches. We hoped that this work would further elucidate the still poorly understood pathogenesis of dermatophytosis and potentially provide targets for genetic testing or new therapies in both animals and humans. We are able to draw two overarching conclusions from this work: 1) Alterations to the Persian cat microbiota do not play an overt role in defense against dermatophyte infection, and 2) a host genetic region containing divergent AMP genes is significantly associated with infection, and our results suggests this alternate AMP allows *Microsporum canis* to establish chronic and extensive infections.

4.1. Limited Involvement of the Microbiota

In the microbiota study, we determined that Persian cat cases exhibited a higher absolute abundance of fungal DNA on the skin than Persian controls, and this correlated with a high relative abundance of *M. canis*, as expected during dermatophyte infection. No other significant alterations were detected between cases and controls or between Persian and non-Persian cats to suggest that other fungal taxa influenced pathogenesis. It is also important to note that *M. canis* was not part of the normal Persian cat microbiota. One shortcoming of this study is that we were not able to fully assess the bacterial microbiota, including staphylococcal species, due to the technical issues described in

section 2.2.3. The study was also not designed to detect differences in metabolites produced by the microbiota. For these reasons, we cannot completely exclude the possibility that the microbiome may play a role in the development of dermatophytosis. Further study of the Persian cat cutaneous microbiome and metabolome, with a particular focus on the bacterial microbiota, is warranted.

4.2. Identification of a Disease-associated Region

After examining the Persian cat microbiota, we performed whole-genome sequencing of Persian cat cases and controls. GWAS performed using the whole-genome data yielded a single locus significantly associated with severe dermatophytosis. This ~1 Mb haplotype contained many genes, but we narrowed our focus to the S100A family region as many of these genes are skin expressed with known antimicrobial properties. In particular, *S100A9* contained an anomalously high number of amino acid substitutions between the case and control haplotypes. S100A8/S100A9 dimerize to form the AMP known as calprotectin, found in immune cells throughout the body as well as within epithelial cells. We further demonstrated that calprotectin is strongly upregulated in the skin during dermatophyte infection thus providing indirect evidence of its involvement in dermatophyte defense. A small number of previous studies have shown a connection between AMPs and dermatophytosis. Jaradat et al. (2015) demonstrated association between susceptibility to typical dermatophytosis and low gene copy number of a skin AMP known as beta-defensin 2 (hBD-2) in humans. Skin AMPs known as cathelicidins showed *in vitro* antifungal activity against dermatophytes and upregulated expression

during infection (Lopez-Garcia et al. 2006). The AMP S100A7 (also known as psoriasin) also exhibited strong *in vitro* antifungal activity against *M. canis* in another study, although hBD2 was shown to have no effect on *M. canis* growth (Fritz et al. 2012). The results of an RNA-seq study showed that, among other genes, *S100A8* and *S100A9* expression were upregulated in the skin of rabbits with dermatophytosis caused by *Trichophyton mentagrophytes* (Xiao et al 2018). While it is accepted in the literature that AMPs play a role in dermatophyte defense, calprotectin has not been specifically implicated or investigated outside of the Xiao et al. (2018) study where upregulated expression was discovered. Further work will be needed to clearly define the signaling pathways in play during infection from the time dermatophytes are sensed by keratinocyte pathogen recognition receptors (PRRs) to upregulation of calprotectin expression.

4.3. S100A9 Evolving Under Balancing Selection

Rather than simply reporting the association identified by GWAS, we sought to investigate this interesting region further—how could there be such impressive divergence in this gene within the Persian breed? By searching for signatures of selection and comparing the sequences of domestic cats and wild felids, we were able to conclude that multiple S100A9 alleles have been maintained in the domestic cat population, an example of balancing selection akin to what is observed with major histocompatibility complex (MHC) alleles and some AMP alleles in various other species. Interestingly, several domestic cat alleles, including the case allele, clustered

most closely with the sand cat, *Felis margarita*, in a highly divergent lineage that branched early in felid evolution. We suspect that this may be the result of ancient hybridization between an unknown, perhaps extinct, wild felid and the ancestor of this sand cat/domestic cat clade. This region may have been introgressed and then maintained via balancing selection, perhaps because certain alleles are better suited to particular pathogens and environments (e.g., arid vs. humid) or because heterozygotes have an advantage against pathogens as they can produce both versions of calprotectin.

4.4. Future Work

Stepping forward from this work, deeper investigation of *S100A9* haplotypes and their pathogen specificities is needed. It would be interesting to further sample wild felid populations and attempt to confirm that ancient hybridization and introgression of an *S100A9* allele is the cause for domestic cat haplotypes H1, H3, H4, and H6 clustering with the sand cat in a divergent S100A lineage. This clade of *S100A9* alleles appears ancient, and yet we see these haplotypes in modern wildcats and domestic cats. Where exactly did this allele come from and what particular pathogens shaped its evolution and encouraged its maintenance? We may need to look beyond cutaneous pathogens, as calprotectin can be found within immune cells (e.g., neutrophils and macrophages) and epithelial cells throughout the body (e.g., intestinal epithelium, epithelium in the lungs). Likewise, we cannot forget that bacteria, viruses, protozoa, and possibly helminths could play a role in shaping calprotectin evolution, as most of these pathogens have proven to be affected in some way by this bountiful antimicrobial protein. For example, if we

consider sand cats and their desert environment, perhaps a protozoal pathogen such as *Leishmania*, spread by sand flies, might place selective pressure on AMP genes. In one study, 4/10 wild-caught sand cats were found to have *Leishmania* amastigotes in the spleen and/or liver, confirming their status as incidental or reservoir hosts of this important zoonotic pathogen (Morsy et al. 1999). Assays could be designed to test the activity of AMPs translated from different haplotypes against a wide range of pathogens, including several species of dermatophytes, bacteria, and perhaps even viruses and protozoa such as *Leishmania* or *Toxoplasma* spp.

Infectious disease pathogenesis necessarily involves both pathogen and host factors. While we focused on host factors for this dissertation research, one could turn to the dermatophyte itself, *M. canis*, for answers. It would be interesting to examine more deeply the population genetics of *M. canis*: How much variation exists within this species of fungus? Are particular strains more virulent? Are particular strains found more often on Persian cats? Are particular strains associated with deep infections (pseudomycetoma)? Overall, what role does fungal genetic variation play in feline infection, or is susceptibility and severity to infection more dependent on host factors such as *S100A9* haplotype alone? Genome assemblies for many dermatophyte species including *M. canis* are publicly available, and these questions could be easily worked on in the future.

Dermatophytic pseudomycetoma is a form of deep dermatophytosis which is essentially confined to the Persian breed, similar to the phenotype examined in this study of chronic, extensive dermatophytosis. It is caused by the same pathogen as chronic,

extensive dermatophytosis but has a different clinical and histologic phenotype. The two cats in this study that had pseudomycetomas (in addition to chronic extensive dermatophytosis) were homozygous for the case haplotype, but this sample size is too limited to determine if the case haplotype is also associated with pseudomycetoma formation. Additional work will be needed to determine if this specific phenotype is also associated with the *S100A9* case haplotype, or if other genetic variants and other immune pathways are at work.

REFERENCES

Abdel-Rahman SM, Preuett BL. 2012. Genetic predictors of susceptibility to cutaneous fungal infections: A pilot genome wide association study to refine a candidate gene search. *J Dermatol Sci* 67:147-152.

Abdel-Rahman SM. 2017. Genetic Predictors of Susceptibility to Dermatophytoses. *Mycopathologia* 182:67-76.

Abraham A, Pedregosa F, Eickenberg M, Gervais P, Mueller A, Kossaifi J, Gramfort A, Thirion B, Varoquaux G. 2014. Machine learning for neuroimaging with scikit-learn. *Front Neuroinform* 8:14.

Abramo F, Vercelli A, Mancianti F. 2001. Two cases of dermatophytic pseudomycetoma in the dog: an immunohistochemical study. *Vet Dermatol* 12:203-207.

Abyzov A, Urban AE, Snyder M, Gerstein M. 2011. CNVnator: An approach to discover, genotype, and characterize typical and atypical CNVs from family and population genome sequencing. *Genome Res* 21:974-984.

Aljabre SH, Richardson MD, Scott EM, Shankland GS. 1992. Germination of Trichophyton mentagrophytes on human stratum corneum in vitro. *J Med Vet Mycol* 30:145-152.

Asz-Sigall D, Lopez-Garcia L, Vega-Memije ME, Lacy-Niebla RM, Garcia-Corona C, Ramirez-Renteria C, Granados J, Villa A, Ameen M, Arenas R. 2010. HLA-DR6 association confers increased resistance to T. rubrum onychomycosis in Mexican Mestizos. *Int J Dermatol* 49:1406-1409.

Baldo A, Mathy A, Tabart J, Camponova P, Vermout S, Massart L, Maréchal F, Galleni M, Mignon B. 2010. Secreted subtilisin Sub3 from Microsporum canis is required for adherence to but not for invasion of the epidermis. *Br J Dermatol* 162:990-997.

Baldo A, Monod M, Mathy A, Cambier L, Bagut ET, Defaweux V, Symoens F, Antoine N, Mignon B. 2012. Mechanisms of skin adherence and invasion by dermatophytes. *Mycoses* 55:218-223.

Benjamini Y, Hochberg Y. 1995. Controlling the False Discovery Rate: A Practical and Powerful Approach to Multiple Testing. *J R Stat Soc Series B Stat Methodol* 57:289-300.

Berg JC, Hamacher KL, Roberts GD. 2007. Pseudomycetoma caused by Microsporum canis in an immunosuppressed patient: a case report and review of the literature. *J Cutan Pathol* 34:431-434.

Besold AN, Culbertson EM, Nam L, Hobbs RP, Boyko A, Maxwell CN, Chazin WJ, Marques AR, Culotta VC. 2018. Antimicrobial action of calprotectin that does not involve metal withholding. *Metallomics* 10:1728-1742.

Bianchi MV, Laisse CJM, Vargas TP, Wouters F, Boabaid FM, Pavarini SP, Ferreiro L, Driemeier D. 2017. Intra-abdominal fungal pseudomycetoma in two cats. *Rev Iberoam Micol* 34:112-115.

Black SS, Abernethy TE, Tyler JW, Thomas MW, Garma-Avina A, Jensen HE. 2001. Intra-abdominal dermatophytic pseudomycetoma in a Persian cat. *J Vet Intern Med* 15:245-248.

Bolyen E, Rideout JR, Dillon MR, Bokulich NA, Abnet CC, Al-Ghalith GA, Alexander H, Alm EJ, Arumugam M, Asnicar F, et al. 2019. Reproducible, interactive, scalable and extensible microbiome data science using QIIME 2. *Nat Biotechnol* 37:852-857.

Bond R, Pocknell AM, Tozet CE. 2001. Pseudomycetoma caused by Microsporum canis in a Persian cat: lack of response to oral terbinafine. *J Small Anim Pract* 42:557-560.

Bongomin F, Gago S, Oladele RO, Denning DW. 2017. Global and Multi-National Prevalence of Fungal Diseases—Estimate Precision. *J Fungus* 3:57.

Bredemeyer KR, Harris AJ, Li G, Zhao L, Foley NM, Roelke-Parker M, O'Brien SJ, Lyons LA, Warren WC, Murphy WJ. 2020. Ultracontinuous Single Haplotype Genome Assemblies for the Domestic Cat (Felis catus) and Asian Leopard Cat (Prionailurus bengalensis). *J Hered* 112:165-173.

Browne K, Chakraborty S, Chen R, Willcox MD, Black DS, Walsh WR, Kumar N. 2020. A New Era of Antibiotics: The Clinical Potential of Antimicrobial Peptides. *Int J Mol Sci* 21:7047.

Burstein VL, Guasconi L, Beccacece I, Theumer MG, Mena C, Prinz I, Cervi L, Herrero M, Masih DT, Chiapello LS. 2018. IL-17-Mediated Immunity Controls Skin Infection and T Helper 1 Response during Experimental Microsporum canis Dermatophytosis. *J Invest Dermatol* 138:1744-1753.

Cagliani R, Fumagalli M, Riva S, Pozzoli U, Comi GP, Menozzi G, Bresolin N, Sironi M. 2008. The signature of long-standing balancing selection at the human defensin beta-1 promoter. *Genome Biol* 9:R143.

Callahan BJ, McMurdie PJ, Rosen MJ, Han AW, Johnson AJ, Holmes SP. 2016. DADA2: High-resolution sample inference from Illumina amplicon data. *Nat Methods* 13:581-583.

Castro-Echeverry E, Fiala K, Fernandez MP. 2017. Dermatophytic Pseudomycetoma of the Scalp. *Am J Dermatopathol* 39:e23-e25.

Chang SC, Liao JW, Shyu CL, Hsu WL, Wong ML. 2011. Dermatophytic pseudomycetomas in four cats. *Vet Dermatol* 22:181-187.

Chapman JR, Hellgren O, Helin AS, Kraus RH, Cromie RL, Waldenström J. 2016. The Evolution of Innate Immune Genes: Purifying and Balancing Selection on β-Defensins in Waterfowl. *Mol Biol Evol* 33:3075-3087.

Chapman JR, Hill T, Unckless RL. 2019. Balancing Selection Drives the Maintenance of Genetic Variation in Drosophila Antimicrobial Peptides. *Genome Biol Evol* 11:2691-2701.

Chessa C, Bodet C, Jousselin C, Wehbe M, Lévêque N, Garcia M. 2020. Antiviral and Immunomodulatory Properties of Antimicrobial Peptides Produced by Human Keratinocytes. *Front Microbiol* 11:1155.

Choi Y, Chan AP. 2015. PROVEAN web server: a tool to predict the functional effect of amino acid substitutions and indels. *Bioinformatics* 31:2745-2747.

Clark HL, Jhingran A, Sun Y, Vareechon C, de Jesus Carrion S, Skaar EP, Chazin WJ, Calera JA, Hohl TM, Pearlman E. 2016. Zinc and manganese chelation by neutrophil S100A8/A9 (calprotectin) limits extracellular Aspergillus fumigatus hyphal growth and corneal infection. *J Immunol* 196:336-344.

Collaborators GBoDS. 2015. Global, regional, and national incidence, prevalence, and years lived with disability for 301 acute and chronic diseases and injuries in 188 countries, 1990-2013: a systematic analysis for the Global Burden of Disease Study 2013. *Lancet* 386:743-800.

Corbin BD, Seeley EH, Raab A, Feldmann J, Miller MR, Torres VJ, Anderson KL, Dattilo BM, Dunman PM, Gerads R, et al. 2008. Metal chelation and inhibition of bacterial growth in tissue abscesses. *Science* 319:962-965.

Corvilain E, Casanova JL, Puel A. 2018. Inherited CARD9 Deficiency: Invasive Disease Caused by Ascomycete Fungi in Previously Healthy Children and Adults. *J Clin Immunol* 38:656-693.

da Costa FV, Farias MR, Bier D, de Andrade CP, de Castro LA, da Silva SC, Ferreiro L. 2013. Genetic variability in Microsporum canis isolated from cats, dogs and humans in Brazil. *Mycoses* 56:582-588.

Das S, De A, Saha R, Sharma N, Khemka M, Singh S, Hesanoor Reja AH, Kumar P. 2020. The Current Indian Epidemic of Dermatophytosis: A Study on Causative Agents and Sensitivity Patterns. *Indian J Dermatol* 65:118-122.

Davis NM, Proctor DM, Holmes SP, Relman DA, Callahan BJ. 2018. Simple statistical identification and removal of contaminant sequences in marker-gene and metagenomics data. *Microbiome* 6:226.

de Hoog GS, Dukik K, Monod M, Packeu A, Stubbe D, Hendrickx M, Kupsch C, Stielow JB, Freeke J, Göker M, et al. 2017. Toward a Novel Multilocus Phylogenetic Taxonomy for the Dermatophytes. *Mycopathologia* 182:5-31.

DeBoer D, Moriello K. 1993. Humoral and cellular immune responses to Microsporum canis in naturally occurring feline dermatophytosis. *Sabouraudia* 31:121-132.

DeBoer DJ, Moriello KA. 1994. Development of an experimental model of Microsporum canis infection in cats. *Vet Microbiol* 42:289-295.

Drummond RA, Gaffen SL, Hise AG, Brown GD. 2014. Innate Defense against Fungal Pathogens. *Cold Spring Harb Perspect Med* 5:a019620.

Drummond RA, Lionakis MS. 2016. Mechanistic Insights into the Role of C-Type Lectin Receptor/CARD9 Signaling in Human Antifungal Immunity. *Front Cell Infect Microbiol* 6:39.

Duangkaew L, Larsuprom L, Kasondorkbua C, Chen C, Chindamporn A. 2017. Cutaneous blastomycosis and dermatophytic pseudomycetoma in a Persian cat from Bangkok, Thailand. *Med Mycol Case Rep* 15:12-15.

Eilbeck K, Quinlan A, Yandell M. 2017. Settling the score: variant prioritization and Mendelian disease. *Nat Rev Genet* 18:599-612.

Ferro S, Vasconi E, Castagnaro M. 2008. A case of intra-abdominal pseudomycetoma in a short hair domestic cat. *Veterinaria* 22:35-41.

Ferwerda B, Ferwerda G, Plantinga TS, Willment JA, van Spriel AB, Venselaar H, Elbers CC, Johnson MD, Cambi A, Huysamen C, et al. 2009. Human dectin-1 deficiency and mucocutaneous fungal infections. *N Engl J Med* 361:1760-1767.

Findley K, Oh J, Yang J, Conlan S, Deming C, Meyer JA, Schoenfeld D, Nomicos E, Park M, Kong HH, et al. 2013. Topographic diversity of fungal and bacterial communities in human skin. *Nature* 498:367-370.

Firat YH, Simanski M, Rademacher F, Schröder L, Brasch J, Harder J. 2014. Infection of Keratinocytes with Trichophytum rubrum Induces Epidermal Growth Factor-Dependent RNase 7 and Human Beta-Defensin-3 Expression. *PLoS One* 9:e93941.

Fritz P, Beck-Jendroschek V, Brasch J. 2012. Inhibition of dermatophytes by the antimicrobial peptides human beta-defensin-2, ribonuclease 7 and psoriasin. *Med Mycol* 50:579-584.

Gallo RL, Nakatsuji T. 2011. Microbial symbiosis with the innate immune defense system of the skin. *J Invest Dermatol* 131:1974-1980.

Gandolfi B, Alhaddad H, Abdi M, Bach LH, Creighton EK, Davis BW, Decker JE, Dodman NH, Ginns EI, Grahn JC, et al. 2018. Applications and efficiencies of the first cat 63K DNA array. *Sci Rep* 8:7024.

García-Romero MT, Granados J, Vega-Memije ME, Arenas R. 2012. Analysis of Genetic Polymorphism of the HLA-B and HLA-DR Loci in Patients with Dermatophytic Onychomycosis and in Their First-Degree Relatives. *Actas Dermosifiliogr* 103:59-62.

Glocker EO, Hennigs A, Nabavi M, Schaffer AA, Woellner C, Salzer U, Pfeifer D, Veelken H, Warnatz K, Tahami F, et al. 2009. A homozygous CARD9 mutation in a family with susceptibility to fungal infections. *N Engl J Med* 361:1727-1735.

Gnat S, Łagowski D, Nowakiewicz A. 2020. Major challenges and perspectives in the diagnostics and treatment of dermatophyte infections. *J Appl Microbiol* 129:212-232.

Gnat S, Łagowski D, Nowakiewicz A. 2021. Genetic Predisposition and its Heredity in the Context of Increased Prevalence of Dermatophytoses. *Mycopathologia* 186:163-176.

Gnat S, Lagowski D, Nowakiewicz A, Zieba P. 2018. Tinea corporis by Microsporum canis in mycological laboratory staff: Unexpected results of epidemiological investigation. *Mycoses* 61:945-953.

Gnat S, Nowakiewicz A, Lagowski D, Zieba P. 2019. Host- and pathogen-dependent susceptibility and predisposition to dermatophytosis. *J Med Microbiol* 68:823-836.

Gohl D, MacLean A, Hauge A, Becker A, Walek D, Beckman K. 2016. An optimized protocol for high-throughput amplicon-based microbiome profiling. *Protoc Exch* 10:978-971.

Gräser Y, Monod M, Bouchara JP, Dukik K, Nenoff P, Kargl A, Kupsch C, Zhan P, Packeu A, Chaturvedi V, et al. 2018. New insights in dermatophyte research. *Med Mycol* 56:2-9.

Grice EA, Segre JA. 2011. The skin microbiome. *Nat Rev Microbiol* 9:244-253.

Grisnik M, Bowers O, Moore AJ, Jones BF, Campbell JR, Walker DM. 2020. The cutaneous microbiota of bats has in vitro antifungal activity against the white nose pathogen. *FEMS Microbiol Ecol* 96:fiz193.

Halldórsdóttir K, Árnason E. 2015. Trans-species polymorphism at antimicrobial innate immunity cathelicidin genes of Atlantic cod and related species. *PeerJ* 3:e976.

Hamm PS, Mueller RC, Kuske CR, Porras-Alfaro A. 2020. Keratinophilic fungi: Specialized fungal communities in a desert ecosystem identified using cultured-based and Illumina sequencing approaches. *Microbiol Res* 239:126530.

Havlickova B, Czaika VA, Friedrich M. 2008. Epidemiological trends in skin mycoses worldwide. *Mycoses* 51:2-15.

Heinen M-P, Cambier L, Antoine N, Gabriel A, Gillet L, Bureau F, Mignon B. 2019. Th1 and Th17 Immune Responses Act Complementarily to Optimally Control Superficial Dermatophytosis. *J Invest Dermatol* 139:626-637.

Hnilica KA, Patterson AP. 2017. Chapter 4 - Fungal Skin Diseases. In. *Small Animal Dermatology (Fourth Edition)*: W.B. Saunders. p. 94-131.

Jaffey JA, Reading NS, Giger U, Abdulmalik O, Buckley RM, Johnstone S, Lyons LA. 2019. Clinical, metabolic, and genetic characterization of hereditary methemoglobinemia caused by cytochrome b5 reductase deficiency in cats. *J Vet Intern Med* 33:2725-2731.

Jaradat SW, Cubillos S, Krieg N, Lehmann K, Issa B, Piehler S, Wehner-Diab S, Hipler UC, Norgauer J. 2015. Low DEFB4 copy number and high systemic hBD-2 and

IL-22 levels are associated with dermatophytosis. *J Invest Dermatol* 135:750-758.

Kang HM, Sul JH, Service SK, Zaitlen NA, Kong SY, Freimer NB, Sabatti C, Eskin E. 2010. Variance component model to account for sample structure in genome-wide association studies. *Nat Genet* 42:348-354.

Kano R, Edamura K, Yumikura H, Maruyama H, Asano K, Tanaka S, Hasegawa A. 2009. Confirmed case of feline mycetoma due to Microsporum canis. *Mycoses* 52:80-83.

Karlsson EK, Baranowska I, Wade CM, Salmon Hillbertz NH, Zody MC, Anderson N, Biagi TM, Patterson N, Pielberg GR, Kulbokas EJ, 3rd, et al. 2007. Efficient mapping of mendelian traits in dogs through genome-wide association. *Nat Genet* 39:1321-1328.

Kipar A, Meli ML, Failing K, Euler T, Gomes-Keller MA, Schwartz D, Lutz H, Reinacher M. 2006. Natural feline coronavirus infection: differences in cytokine patterns in association with the outcome of infection. *Vet Immunol Immunopathol* 112:141-155.

Korneliussen TS, Albrechtsen A, Nielsen R. 2014. ANGSD: Analysis of Next Generation Sequencing Data. *BMC Bioinformatics* 15:356.

Langan EA, Kunstner A, Miodovnik M, Zillikens D, Thaci D, Baines JF, Ibrahim SM, Solbach W, Knobloch JK. 2019. Combined culture and metagenomic analyses reveal significant shifts in the composition of the cutaneous microbiome in psoriasis. *Br J Dermatol* 181:1254-1264.

Lanternier F, Pathan S, Vincent QB, Liu L, Cypowyj S, Prando C, Migaud M, Taibi L, Ammar-Khodja A, Boudghene Stambouli O, et al. 2013. Deep dermatophytosis and inherited CARD9 deficiency. *N Engl J Med* 369:1704-1714.

Lazzaro BP, Zasloff M, Rolff J. 2020. Antimicrobial peptides: Application informed by evolution. *Science* 368:eaau5480.

Lewis DT, Foil CS, Hosgood G. 1991. Epidemiology and Clinical Features of Dermatophytosis in Dogs and Cats at Louisiana State University: 1981–1990. *Vet Dermatol* 2:53-58.

Li G, Davis BW, Eizirik E, Murphy WJ. 2016. Phylogenomic evidence for ancient hybridization in the genomes of living cats (Felidae). *Genome Res* 26:1-11.

Li G, Figueiró HV, Eizirik E, Murphy WJ. 2019. Recombination-Aware Phylogenomics Reveals the Structured Genomic Landscape of Hybridizing Cat Species. *Mol Biol and Evol* 36:2111-2126.

Li G, Hillier LW, Grahn RA, Zimin AV, David VA, Menotti-Raymond M, Middleton R, Hannah S, Hendrickson S, Makunin A, et al. 2016. A High-Resolution SNP Array-Based Linkage Map Anchors a New Domestic Cat Draft Genome Assembly and Provides Detailed Patterns of Recombination. *G3* 6:1607-1616.

Li H. 2013. Aligning sequence reads, clone sequences and assembly contigs with BWA-MEM. arXiv:1303.3997.

Li H, Bouchara j-p, Hsu M, Barton R, Su S, Chang T. 2008. Identification of dermatophytes by sequence analysis of the rRNA gene internal transcribed spacer regions. *J Med Microbiol* 57:592-600.

Liu X, Tan J, Yang H, Gao Z, Cai Q, Meng L, Yang L. 2019. Characterization of Skin Microbiome in Tinea Pedis. *Indian J Microbiol* 59:422-427.

López-García B, Lee PHA, Gallo RL. 2006. Expression and potential function of cathelicidin antimicrobial peptides in dermatophytosis and tinea versicolor. *J Antimicrob Chemother* 57:877-882.

Luo Z, Wu Y, Zhang WX, Wang L, Zuo F, Zhang GW. 2018. Nonsynonymous DNA variation in the functional domain of the S100A7, -A8, -A9 genes in taurine cattle and yak. *Anim Genet* 49:351-353.

Lyons LA. 2019. 99 Lives. *Lyons Feline Comparative Genetics*:http://felinegenetics.missouri.edu/99lives.

Marodi L, Erdos M. 2010. Dectin-1 Deficiency and Mucocutaneous Fungal Infections. *N Engl J Med* 362:367-368.

Marsilio S, Kleinschmidt S, Nolte I, Hewicker-Trautwein M. 2014. Immunohistochemical and Morphometric Analysis of Intestinal Full-thickness Biopsy Samples from Cats with Lymphoplasmacytic Inflammatory Bowel Disease. *J Comp Pathol* 150:416-423.

Martin M. 2011. Cutadapt removes adapter sequences from high-throughput sequencing reads. *EMBnet.journal* 17:3.

Mauler DA, Gandolfi B, Reinero CR, O'Brien DP, Spooner JL, Lyons LA. 2017. Precision Medicine in Cats: Novel Niemann-Pick Type C1 Diagnosed by Whole-Genome Sequencing. *J Vet Intern Med* 31:539-544.

Meason-Smith C, Diesel A, Patterson AP, Older CE, Johnson TJ, Mansell J, Suchodolski JS, Rodrigues Hoffmann A. 2017. Characterization of the cutaneous mycobiota in healthy and allergic cats using next generation sequencing. *Vet Dermatol* 28:71-e17.

Meason-Smith C, Diesel A, Patterson AP, Older CE, Mansell JM, Suchodolski JS, Rodrigues Hoffmann A. 2015. What is living on your dog's skin? Characterization of the canine cutaneous mycobiota and fungal dysbiosis in canine allergic dermatitis. *FEMS Microbiol Ecol* 91:fiv139.

Merkhofer RM, Klein BS. 2020. Advances in Understanding Human Genetic Variations That Influence Innate Immunity to Fungi. *Front Cell Infect Microbiol* 10:69.

Miller RI. 2010. Nodular granulomatous fungal skin diseases of cats in the United Kingdom: a retrospective review. *Vet Dermatol* 21:130-135.

Miller WH, Muller GH, Scott DW, Griffin CE, Campbell KL. 2013. *Muller and Kirk's Small Animal Dermatology*. St. Louis, Mo: Saunders.

Minh BQ, Schmidt HA, Chernomor O, Schrempf D, Woodhams MD, von Haeseler A, Lanfear R. 2020. IQ-TREE 2: New Models and Efficient Methods for Phylogenetic Inference in the Genomic Era. *Mol Biol and Evol* 37:1530-1534.

Mohsen A, Park J, Chen Y-A, Kawashima H, Mizuguchi K. 2019. Impact of quality trimming on the efficiency of reads joining and diversity analysis of Illumina paired-end reads in the context of QIIME1 and QIIME2 microbiome analysis frameworks. *BMC Bioinformatics* 20:581.

Mookherjee N, Anderson MA, Haagsman HP, Davidson DJ. 2020. Antimicrobial host defence peptides: functions and clinical potential. *Nat Rev Drug Discov* 19:311-332.

Morgulis A, Gertz EM, Schäffer AA, Agarwala R. 2006. WindowMasker: window-based masker for sequenced genomes. *Bioinformatics* 22:134-141.

Moriello KA. 1991. Fungal flora of the haircoat of cats with and without dermatophytosis. *J Med Vet Mycol* 29:285-292.

Moriello KA, Coyner K, Paterson S, Mignon B. 2017. Diagnosis and treatment of dermatophytosis in dogs and cats.: Clinical Consensus Guidelines of the World Association for Veterinary Dermatology. *Vet Dermatol* 28:266-e268.

Morsy TA, Al-Dakhil MA, El-Bahrawy AF. 1999. Natural Lieshmania infection in sand cats captured in Riyadh district, Saudi Arabia. *J Egypt Soc Parasitol* 29:69-74.

Myers AN, Older CE, Diesel AB, Lawhon SD, Rodrigues Hoffmann A. 2021. Characterization of the cutaneous mycobiota in Persian cats with severe dermatophytosis. *Vet Dermatol*. doi: 10.1111/vde.12969.

Narang T, Bhattacharjee R, Singh S, Jha K, Kavita, Mahajan R, Dogra S. 2019. Quality of life and psychological morbidity in patients with superficial cutaneous dermatophytosis. *Mycoses* 62:680-685.

Nardoni S, Franceschi A, Mancianti F. 2007. Identification of Microsporum canis from dermatophytic pseudomycetoma in paraffin-embedded veterinary specimens using a common PCR protocol. *Mycoses* 50:215-217.

Nenoff P, Verma SB, Vasani R, Burmester A, Hipler U-C, Wittig F, Krüger C, Nenoff K, Wiegand C, Saraswat A, et al. 2019. The current Indian epidemic of superficial dermatophytosis due to Trichophyton mentagrophytes—A molecular study. *Mycoses* 62:336-356.

Nielsen J, Kofod-Olsen E, Spaun E, Larsen CS, Christiansen M, Mogensen TH. 2015. A STAT1-gain-of-function mutation causing Th17 deficiency with chronic mucocutaneous candidiasis, psoriasiform hyperkeratosis and dermatophytosis. *BMJ Case Rep* 2015.

Nilsson RH, Larsson K-H, Taylor AF S, Bengtsson-Palme J, Jeppesen TS, Schigel D, Kennedy P, Picard K, Glöckner FO, Tedersoo L, et al. 2018. The UNITE database for molecular identification of fungi: handling dark taxa and parallel taxonomic classifications. *Nucleic Acids Res* 47:D259-D264.

Nitta C, Taborda C, Santana A, Larsson C, Daniel A. 2016. Isolation of Dermatophytes from the Hair Coat of Healthy Persian Cats without Skin Lesions from Commercial Catteries Located in São Paulo Metropolitan Area, Brazil. *Acta Sci Vet* 44:0.

Nobre Mde O, Negri Mueller E, Teixeira Tillmann M, da Silva Rosa C, Normanton Guim T, Vives P, Fernandes M, Madrid IM, Fernandes CG, Meireles MC. 2010. Disease progression of dermatophytic pseudomycetoma in a Persian cat. *Rev Iberoam Micol* 27:98-100.

Noel AC, Hu DL. 2018. Cats use hollow papillae to wick saliva into fur. *Proc Natl Acad Sci U S A* 115:12377.

Nuttall TJ, German AJ, Holden SL, Hopkinson C, McEwan NA. 2008. Successful resolution of dermatophyte mycetoma following terbinafine treatment in two cats. *Vet Dermatol* 19:405-410.

Oh A, Pearce JW, Gandolfi B, Creighton EK, Suedmeyer WK, Selig M, Bosiack AP, Castaner LJ, Whiting RE, Belknap EB, et al. 2017. Early-Onset Progressive Retinal Atrophy Associated with an IQCB1 Variant in African Black-Footed Cats (Felis nigripes). *Sci Rep* 7:43918.

Oksanen J, Blanchet FG, Friendly M, Kindt R, Legendre P, McGlinn D, Minchin PR, O'Hara RB, Simpson GL, Solymos P, et al. 2019. vegan: Community Ecology Package. R package version 2.5-6.https://CRAN.R-project.org/package=vegan.

Older CE, Diesel AB, Lawhon SD, Queiroz CRR, Henker LC, Rodrigues Hoffmann A. 2019. The feline cutaneous and oral microbiota are influenced by breed and environment. *PLoS One* 14:e0220463.

Ontiveros ES, Ueda Y, Harris SP, Stern JA. 2019. Precision medicine validation: identifying the MYBPC3 A31P variant with whole-genome sequencing in two Maine Coon cats with hypertrophic cardiomyopathy. *J Feline Med Surg* 21:1086-1093.

Patel NH, Padhiyar JK, Patel AP, Chhebber AS, Patel BR, Patel TD. 2020. Psychosocial and Financial Impact of Disease among Patients of Dermatophytosis, a Questionnaire-Based Observational Study. *Indian Dermatol Online J* 11:373-377.

Poplin R, Ruano-Rubio V, DePristo MA, Fennell TJ, Carneiro MO, Van der Auwera GA, Kling DE, Gauthier LD, Levy-Moonshine A, Roazen D, et al. 2018. Scaling accurate genetic variant discovery to tens of thousands of samples. *bioRxiv*:201178.

Quast C, Pruesse E, Yilmaz P, Gerken J, Schweer T, Yarza P, Peplies J, Glöckner FO. 2012. The SILVA ribosomal RNA gene database project: improved data processing and web-based tools. *Nucleic Acids Res* 41:D590-D596.

Reis APC, Correia FF, Jesus TM, Pagliari C, Sakai-Valente NY, Belda Junior W, Criado PR, Benard G, Sousa MGT. 2019. In situ immune response in human dermatophytosis: possible role of Langerhans cells (CD1a+) as a risk factor for dermatophyte infection. *Rev Inst Med Trop Sao Paulo* 61:e56.

Robinson JT, Thorvaldsdóttir H, Wenger AM, Zehir A, Mesirov JP. 2017. Variant Review with the Integrative Genomics Viewer. *Cancer Res* 77:e31-e34.

Rouzaud C, Hay R, Chosidow O, Dupin N, Puel A, Lortholary O, Lanternier F. 2015. Severe Dermatophytosis and Acquired or Innate Immunodeficiency: A Review. *J Fungi* 2:4.

Sadahiro A, Moraes JRF, Moraes MEH, Romero M, Gouvea NAdL, Gouvea CJ, Ogusku MM, Campbell I, Zaitz C. 2004. HLA in Brazilian Ashkenazic Jews with chronic dermatophytosis caused by Trichophyton rubrum. *Braz J Microbiol* 35:69-73.

Salter SJ, Cox MJ, Turek EM, Calus ST, Cookson WO, Moffatt MF, Turner P, Parkhill J, Loman NJ, Walker AW. 2014. Reagent and laboratory contamination can critically impact sequence-based microbiome analyses. *BMC Biol* 12:87.

Sander MA, Sander MS, Isaac-Renton JL, Croxen MA. 2019. The Cutaneous Microbiome: Implications for Dermatology Practice. *J Cutan Med Surg* 23:436-441.

Saunte DML, Pereiro-Ferreirós M, Rodríguez-Cerdeira C, Sergeev AY, Arabatzis M, Prohić A, Piraccini BM, Lecerf P, Nenoff P, Kotrekhova LP, et al. 2021. Emerging antifungal treatment failure of dermatophytosis in Europe: take care or it may become endemic. *J Eur Acad Dermatol Venereol* 35:1582-1586.

Sawada Y, Nakamura M, Kabashima-Kubo R, Shimauchi T, Kobayashi M, Tokura Y. 2013. Defective epidermal induction of S100A7/psoriasin associated with low frequencies of skin-infiltrating Th17 cells in dermatophytosis-prone adult T cell leukemia/lymphoma. *Clin Immunol* 148:1-3.

Scott DW, Miller Jr WH, Griffin CE. 2001. Chapter 5 - Fungal Skin Diseases. In. *Muller & Kirk's Small Animal Dermatology (Sixth Edition)*. Philadelphia: W.B. Saunders. p. 336-422.

Segata N, Izard J, Waldron L, Gevers D, Miropolsky L, Garrett WS, Huttenhower C. 2011. Metagenomic biomarker discovery and explanation. *Genome Biol* 12:R60.

Serjeantson S, Lawrence G. 1977. Autosomal recessive inheritance of susceptibility to tinea imbricata. *Lancet* 1:13-15.

Siewert KM, Voight BF. 2017. Detecting Long-Term Balancing Selection Using Allele Frequency Correlation. *Mol Biol Evol* 34:2996-3005.

Smeekens SP, Huttenhower C, Riza A, van de Veerdonk FL, Zeeuwen PL, Schalkwijk J, van der Meer JW, Xavier RJ, Netea MG, Gevers D. 2014. Skin microbiome imbalance in patients with STAT1/STAT3 defects impairs innate host defense responses. *J Innate Immun* 6:253-262.

Sohnle PG, Collins-Lech C, Wiessner JH. 1991. The zinc-reversible antimicrobial activity of neutrophil lysates and abscess fluid supernatants. *J Infect Dis* 164:137-142.

Souza PFN, Marques LSM, Oliveira JTA, Lima PG, Dias LP, Neto NAS, Lopes FES, Sousa JS, Silva AFB, Caneiro RF, et al. 2020. Synthetic antimicrobial peptides: From choice of the best sequences to action mechanisms. *Biochimie* 175:132-145.

Sparber F, LeibundGut-Landmann S. 2018. IL-17 Takes Center Stage in Dermatophytosis. *J Invest Dermatol* 138:1691-1693.

Stacy A, Belkaid Y. 2019. Microbial guardians of skin health. *Science* 363:227-228.

Stanley SW, Fischetti AJ, Jensen HE. 2008. Imaging diagnosis--sublumbar pseudomycetoma in a Persian cat. *Vet Radiol Ultrasound* 49:176-178.

Steinbakk M, Naess-Andresen CF, Lingaas E, Dale I, Brandtzaeg P, Fagerhol MK. 1990. Antimicrobial actions of calcium binding leucocyte L1 protein, calprotectin. *Lancet* 336:763-765.

Thian A, Woodgyer AJ, Holloway SA. 2008. Dysgonic strain of Microsporum canis pseudomycetoma in a Domestic Long-hair cat. *Aust Vet J* 86:324-328.

Urban CF, Ermert D, Schmid M, Abu-Abed U, Goosmann C, Nacken W, Brinkmann V, Jungblut PR, Zychlinsky A. 2009. Neutrophil extracellular traps contain calprotectin, a cytosolic protein complex involved in host defense against Candida albicans. *PLoS Pathog* 5:e1000639.

Vaezi A, Fakhim H, Abtahian Z, Khodavaisy S, Geramishoar M, Alizadeh A, Meis JF, Badali H. 2018. Frequency and Geographic Distribution of CARD9 Mutations in Patients With Severe Fungal Infections. *Front Microbiol* 9:2434.

van de Veerdonk FL, Plantinga TS, Hoischen A, Smeekens SP, Joosten LAB, Gilissen C, Arts P, Rosentul DC, Carmichael AJ, Smits-van der Graaf CAA, et al. 2011. STAT1 Mutations in Autosomal Dominant Chronic Mucocutaneous Candidiasis. *N Engl J Med* 365:54-61.

Vázquez-Baeza Y, Gonzalez A, Smarr L, McDonald D, Morton JT, Navas-Molina JA, Knight R. 2017. Bringing the Dynamic Microbiome to Life with Animations. *Cell Host Microbe* 21:7-10.

Vázquez-Baeza Y, Pirrung M, Gonzalez A, Knight R. 2013. EMPeror: a tool for visualizing high-throughput microbial community data. *Gigascience* 2:16.

Walch G, Knapp M, Rainer G, Peintner U. 2016. Colony-PCR Is a Rapid Method for DNA Amplification of Hyphomycetes. *J Fungi* 2:12.

Wang R, Song Y, Du M, Yang E, Yu J, Wan Z, Li R. 2018. Skin microbiome changes in patients with interdigital tinea pedis. *Br J Dermatol* 179:965-968.

Weitzman I, Summerbell RC. 1995. The dermatophytes. *Clin Microbiol Rev* 8:240-259.

Wisal AG, Salim M. 2010. Isolation and identification of dermatophytes from infected Camels. *Sudan J Vet Res* 25:49-53.

Wu Y, Yang J, Yang F, Liu T, Leng W, Chu Y, Jin Q. 2009. Recent dermatophyte divergence revealed by comparative and phylogenetic analysis of mitochondrial genomes. *BMC Genomics* 10:238.

Xiao W, He H, Tong Y, Cai M, Shi Y, Liu B, Wang J, Qin Y, Lai S. 2018. Transcriptome analysis of Trichophyton mentagrophytes–induced rabbit (Oryctolagus cuniculus) dermatophytosis. *Microb Pathog* 114:350-356.

Yager JA, Wilcock BP, Lynch JA, Thompson AR. 1986. Mycetoma-like granuloma in a cat caused by Microsporum canis. *J Comp Pathol* 96:171-176.

Yamaguchi N, Driscoll CA, Kitchner AC, Ward JM, Macdonald DW. 2004. Craniological differentiation between European wildcats (Felis silvestris silvestris), African wildcats (F. s. lybica) and Asian wildcats (F. s. ornata): implications for their evolution and conservation. *Biol J Linn Soc* 83:47-63.

Zafrany A, Ben-Oz J, Segev G, Milgram J, Zemer O, Jensen HE, Kelmer E. 2014. Successful treatment of an intra-pelvic fungal pseudomycetoma causing constipation and hypercalcaemia in a Persian cat. *J Feline Med Surg* 16:369-372.

Zheng H, Blechert O, Mei H, Ge L, Liu J, Tao Y, Li D, de Hoog GS, Liu W. 2020. Assembly and analysis of the whole genome of Arthroderma uncinatum strain T10, compared with Microsporum canis and Trichophyton rubrum. *Mycoses* 63:683-693.

Zhou X, Stephens M. 2012. Genome-wide efficient mixed-model analysis for association studies. *Nat Genet* 44:821-824.

Zimmerman K, Feldman B, Robertson J, Herring ES, Manning T. 2003. Dermal mass aspirate from a Persian cat. *Vet Clin Pathol* 32:213-217.

Zygiel EM, Nolan EM. 2018. Transition Metal Sequestration by the Host-Defense Protein Calprotectin. *Annu Rev Biochem* 87:621-643.

APPENDIX A

SUPPLEMENTARY TABLES

Table S1. Column definitions for Table S2.

Table S2 metadata column name	definition
sample-id	full sample ID
sample-name	brief sample name
sample-VS-control	true sample swab OR negative control swab
swab-type	type of swab
case-VS-control	general/lesion swab from affected cat OR general swab from control cat
case-VS-control-groups	general/lesion swab from affected cat OR general swab from various control cat groups
lesion-VS-control	lesion swab OR general swab from control cat
lesion-VS-general	lesion swab OR general swab from affected cat
breed	breed of cat
cat-VS-environ	sample collected from a cat OR collected from household environment
environ-case-VS-environ-control	environmental sample from affected cat household OR environmental sample from control cat household
household-id	ID of household sample was collected from (no more than three cats were enrolled from one household)
age	age at time of sample collection
sex	sex
geography-by-state	geographical location of sample collection, by state
geography-by-country	geographical location of sample collection, by country
collector-id	ID of veterinarian collecting the sample
pseudomycetoma	history of dermatophytic pseudomycetoma
1mo-steroids	steroids administerd to patient within one month of sample collection
1mo-antifungals	antifungals administered to patient within one month of sample collection
chronic-upper-resp	patient diagnosed with chronic upper respiratory tract disease at time of sample collection

S2 Table. Sample metadata for the microbiota study, as needed for QIIME2 data analysis (Section 2).

sample-id	sample-name	sample-VS-control	swab-type	case-VS-control	case-VS-control-groups	lesion-VS-control	lesion-VS-general
Persian_G1_general_1G	1G	sample	general	control	control_naive	control	
Persian_G1_general_2G	2G	sample	general	control	control_naive	control	
Persian_G1_general_3G	3G	sample	general	control	control_naive	control	
Persian_G1_general_4G	4G	sample	general	control	control_naive	control	
Persian_G1_general_5G	5G	sample	general	control	control_naive	control	
Persian_G1_general_6G	6G	sample	general	control	control_naive	control	
Persian_G1_general_7G	7G	sample	general	control	control_naive	control	
Persian_G1_general_8G	8G	sample	general	control	control_naive	control	
Persian_G1_general_9G	9G	sample	general	control	control_naive	control	
Persian_G1_general_10G	10G	sample	general	control	control_naive	control	
Persian_G1_general_11G	11G	sample	general	control	control_naive	control	
Persian_G2_general_12G	12G	sample	general	control	control_resistant	control	
Persian_G2_general_13G	13G	sample	general	control	control_resistant	control	
Persian_G2_general_14G	14G	sample	general	control	control_resistant	control	
Persian_G2_general_15G	15G	sample	general	control	control_resistant	control	
Persian_G2_general_16G	16G	sample	general	control	control_resistant	control	
Persian_G2_general_17G	17G	sample	general	control	control_resistant	control	
Persian_G2_general_18G	18G	sample	general	control	control_resistant	control	
Persian_G2_general_19G	19G	sample	general	control	control_resistant	control	
DLH_general_20G	20G	sample	general	control	DLH_control	control	
DLH_general_21G	21G	sample	general	control	DLH_control	control	
DLH_general_22G	22G	sample	general	control	DLH_control	control	
DLH_general_23G	23G	sample	general	control	DLH_control	control	
DLH_general_24G	24G	sample	general	control	DLH_control	control	
DLH_general_25G	25G	sample	general	control	DLH_control	control	
DLH_general_26G	26G	sample	general	control	DLH_control	control	
DLH_general_27G	27G	sample	general	control	DLH_control	control	
DLH_general_28G	28G	sample	general	control	DLH_control	control	
DLH_general_29G	29G	sample	general	control	DLH_control	control	
Persian_G3_general_30G	30G	sample	general	case	case		general
Persian_G3_general_31G	31G	sample	general	case	case		general
Persian_G3_lesion_32G	32G	sample	general	case	case		general
Persian_G3_general_33G	33G	sample	general	case	case		general
Persian_G3_general_34G	34G	sample	general	case	case		general
Persian_G3_general_35G	35G	sample	general	case	case		general
Persian_G3_general_36G	36G	sample	general	case	case		general
Persian_G3_lesion_30L	30L	sample	lesion	case	case	lesion	lesion
Persian_G3_lesion_31L	31L	sample	lesion	case	case	lesion	lesion
Persian_G3_general_32L	32L	sample	lesion	case	case	lesion	lesion
Persian_G3_lesion_33L	33L	sample	lesion	case	case	lesion	lesion
Persian_G3_lesion_34L	34L	sample	lesion	case	case	lesion	lesion
Persian_G3_lesion_36L	36L	sample	lesion	case	case	lesion	lesion
Persian_G1_environ_1E	1E	sample	environ				
Persian_G1_environ_2E	2E	sample	environ				
Persian_G1_environ_4E	4E	sample	environ				
Persian_G1_environ_6E	6E	sample	environ				
Persian_G1_environ_7E	7E	sample	environ				
Persian_G1_environ_8E	8E	sample	environ				
Persian_G1_environ_10E	10E	sample	environ				
Persian_G1_environ_11E	11E	sample	environ				
Persian_G2_environ_14E	14E	sample	environ				
Persian_G2_environ_18E	18E	sample	environ				
Persian_G2_environ_19E	19E	sample	environ				
Persian_G3_environ_30E	30E	sample	environ				
Persian_G3_environ_36E	36E	sample	environ				
Control_Reagent	Reagent	control					
Control_Swab	Swab	control					

S2 Table. Continued.

sample-id	breed	cat-VS-environ	environ-case-VS-environ-control	household-id	age	sex	geography-by-state	geography-by-country
Persian_G1_general_1G	Persian	cat		1	1-5	M	TX	USA
Persian_G1_general_2G	Persian	cat		6	>10	F	TX	USA
Persian_G1_general_3G	Persian	cat		9	>10	F	TX	USA
Persian_G1_general_4G	Persian	cat		7	6-10	M	TX	USA
Persian_G1_general_5G	Persian	cat		10	1-5	M	TX	USA
Persian_G1_general_6G	Persian	cat		5	1-5	F	TX	USA
Persian_G1_general_7G	Persian	cat		8	>10	M	TX	USA
Persian_G1_general_8G	Persian	cat		3	>10	M	TX	USA
Persian_G1_general_9G	Persian	cat		11	1-5	M	TX	USA
Persian_G1_general_10G	Persian	cat		2	>10	F	TX	USA
Persian_G1_general_11G	Persian	cat		4	>10	F	TX	USA
Persian_G2_general_12G	Persian	cat		14	>10	M	LA	USA
Persian_G2_general_13G	Persian	cat		14	>10	M	TX	USA
Persian_G2_general_14G	Persian	cat		12	1-5	F	TX	USA
Persian_G2_general_15G	Persian	cat		15	6-10	M	TX	USA
Persian_G2_general_16G	Persian	cat		15	6-10	F	TX	USA
Persian_G2_general_17G	Persian	cat		34	6-10	F	Oman	Oman
Persian_G2_general_18G	Persian	cat		6	1-5	M	TX	USA
Persian_G2_general_19G	Persian	cat		13	6-10	M	TX	USA
DLH_general_20G	DLH	cat		24	1-5	F	TX	USA
DLH_general_21G	DLH	cat		25	1-5	F	TX	USA
DLH_general_22G	DLH	cat		26	6-10	M	TX	USA
DLH_general_23G	DLH	cat		27	>10	F	TX	USA
DLH_general_24G	DLH	cat		28	>10	F	TX	USA
DLH_general_25G	DLH	cat		29	1-5	M	TX	USA
DLH_general_26G	DLH	cat		30	1-5	M	TX	USA
DLH_general_27G	DLH	cat		31	6-10	M	TX	USA
DLH_general_28G	DLH	cat		32	>10	F	TX	USA
DLH_general_29G	DLH	cat		33	1-5	M	TX	USA
Persian_G3_general_30G		cat		16	>10	M	TX	USA
Persian_G3_general_31G		cat		15	6-10	F	TX	USA
Persian_G3_lesion_32G		cat		20	1-5	F	Italy	Italy
Persian_G3_general_33G		cat		21	6-10	F	Italy	Italy
Persian_G3_general_34G		cat		22	6-10	M	Italy	Italy
Persian_G3_general_35G		cat		23	1-5	F	Estonia	Estonia
Persian_G3_general_36G		cat		19	6-10	M	CT	USA
Persian_G3_lesion_30L		cat		16	>10	M	TX	USA
Persian_G3_lesion_31L		cat		15	6-10	F	TX	USA
Persian_G3_general_32L		cat		20	1-5	F	Italy	Italy
Persian_G3_lesion_33L		cat		21	6-10	F	Italy	Italy
Persian_G3_lesion_34L		cat		22	6-10	M	Italy	Italy
Persian_G3_lesion_36L		cat		19	6-10	M	CT	USA
Persian_G1_environ_1E		environ	env_control	1	1-5	M		
Persian_G1_environ_2E		environ	env_control	6	>10	F		
Persian_G1_environ_4E		environ	env_control	7	6-10	M		
Persian_G1_environ_6E		environ	env_control	5	1-5	F		
Persian_G1_environ_7E		environ	env_control	8	>10	M		
Persian_G1_environ_8E		environ	env_control	3	>10	M		
Persian_G1_environ_10E		environ	env_control	2	>10	F		
Persian_G1_environ_11E		environ	env_control	4	>10	F		
Persian_G2_environ_14E		environ	env_control	12	1-5	F		
Persian_G2_environ_18E		environ	env_control	6	1-5	M		
Persian_G2_environ_19E		environ	env_control	13	6-10	M		
Persian_G3_environ_30E		environ	env_case	16	>10	M		
Persian_G3_environ_36E		environ	env_case	19	6-10	M		
Control_Reagent								
Control_Swab								

S2 Table. Continued.

sample-id	collector-id	pseudomycetoma	1mo-steroids	1mo-antifungals	chronic-upper-resp
Persian_G1_general_1G	D	no	no	no	yes
Persian_G1_general_2G	B	no	no	no	yes
Persian_G1_general_3G	I	no	yes	no	no
Persian_G1_general_4G	B	no	no	no	yes
Persian_G1_general_5G	A	no	no	no	no
Persian_G1_general_6G	B	no	no	no	no
Persian_G1_general_7G	B	no	no	no	yes
Persian_G1_general_8G	B	no	no	no	yes
Persian_G1_general_9G	B	no	no	no	no
Persian_G1_general_10G	B	no	no	no	no
Persian_G1_general_11G	B	no	no	no	no
Persian_G2_general_12G	A	no	no	no	yes
Persian_G2_general_13G	A	no	no	no	no
Persian_G2_general_14G	D	no	no	no	yes
Persian_G2_general_15G	B	no	no	no	no
Persian_G2_general_16G	B	no	no	no	no
Persian_G2_general_17G	H	no	no	no	no
Persian_G2_general_18G	B	no	no	no	no
Persian_G2_general_19G	B	no	no	no	yes
DLH_general_20G	A	no	no	no	no
DLH_general_21G	A	no	no	no	no
DLH_general_22G	A	no	no	no	no
DLH_general_23G	A	no	no	no	no
DLH_general_24G	A	no	no	no	no
DLH_general_25G	A	no	no	no	no
DLH_general_26G	A	no	no	no	no
DLH_general_27G	A	no	no	no	no
DLH_general_28G	A	no	no	no	no
DLH_general_29G	J	no	no	no	no
Persian_G3_general_30G	A	no	no	no	yes
Persian_G3_general_31G	B	no	no	no	no
Persian_G3_lesion_32G	E	no	no	yes	no
Persian_G3_general_33G	E	no	no	no	no
Persian_G3_general_34G	E	yes	no	no	no
Persian_G3_general_35G	G	no	no	yes	no
Persian_G3_general_36G	F	yes	no	yes	no
Persian_G3_lesion_30L	A	no	no	no	yes
Persian_G3_lesion_31L	B	no	no	no	no
Persian_G3_general_32L	E	no	no	yes	no
Persian_G3_lesion_33L	E	no	no	no	no
Persian_G3_lesion_34L	E	yes	no	no	no
Persian_G3_lesion_36L	F	yes	no	yes	no
Persian_G1_environ_1E	D	no	no	no	yes
Persian_G1_environ_2E	B	no	no	no	yes
Persian_G1_environ_4E	B	no	no	no	yes
Persian_G1_environ_6E	B	no	no	no	no
Persian_G1_environ_7E	B	no	no	no	yes
Persian_G1_environ_8E	B	no	no	no	yes
Persian_G1_environ_10E	B	no	no	no	no
Persian_G1_environ_11E	B	no	no	no	no
Persian_G2_environ_14E	D	no	no	no	yes
Persian_G2_environ_18E	B	no	no	no	no
Persian_G2_environ_19E	B	no	no	no	yes
Persian_G3_environ_30E	A	no	no	no	yes
Persian_G3_environ_36E	F	yes	no	yes	no
Control_Reagent					
Control_Swab					